

1,4-Oxazine β -Secretase 1 (BACE1) Inhibitors: From Hit Generation to Orally Bioavailable Brain Penetrant Leads

Frederik J. R. Rombouts,*[†] Gary Tresadern,[#] Oscar Delgado,[‡] Carolina Martínez-Lamenca,[†] Michiel Van Gool,[‡] Aránzazu García-Molina,[‡] Sergio A. Alonso de Diego,[‡] Daniel Oehlrich,[†] Hana Prokopcova,[†] José Manuel Alonso,[#] Nigel Austin,^{||} Herman Borghys,^{||} Sven Van Brandt,[†] Michel Surkyn,[†] Michel De Cleyn,[†] Ann Vos,^{||} Richard Alexander,[⊥] Gregor Macdonald,[†] Dieder Moechars,[§] Harrie Gijsen,[†] and Andrés A. Trabanco*,[‡]

*Neuroscience Medicinal Chemistry, Janssen Research & Development, Janssen Pharmaceutica NV, Turnhoutseweg 30, B-2340 Beerse, Belgium

[†]Neuroscience Medicinal Chemistry, Janssen Research & Development, Janssen–Cilag SA, C/Jarama 75A, 45007 Toledo, Spain

[§]Neuroscience Biology, Janssen Research & Development, Janssen Pharmaceutica NV, Turnhoutseweg 30, B-2340 Beerse, Belgium

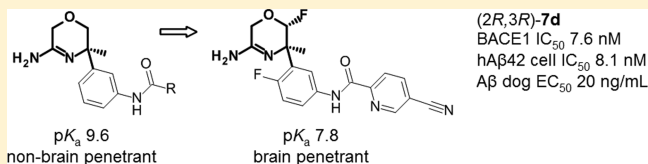
^{||}Discovery Sciences, Janssen Research & Development, Janssen Pharmaceutica NV, Turnhoutseweg 30, B-2340 Beerse, Belgium

[⊥]Biologics Research, Janssen Research & Development, 1400 McKean Road, Spring House, Pennsylvania 19477, United States

[#]Discovery Sciences, Janssen Research & Development, Janssen–Cilag SA, C/Jarama 75A, 45007 Toledo, Spain

S Supporting Information

ABSTRACT: 1,4-Oxazines are presented, which show good in vitro inhibition in enzymatic and cellular BACE1 assays. We describe lead optimization focused on reducing the amidine pK_a while optimizing interactions in the BACE1 active site. Our strategy permitted modulation of properties such as permeation and especially P-glycoprotein efflux. This led to compounds which were orally bioavailable, centrally active, and which demonstrated robust lowering of brain and CSF A β levels, respectively, in mouse and dog models. The amyloid lowering potential of these molecules makes them valuable leads in the search for new BACE1 inhibitors for the treatment of Alzheimer's disease.



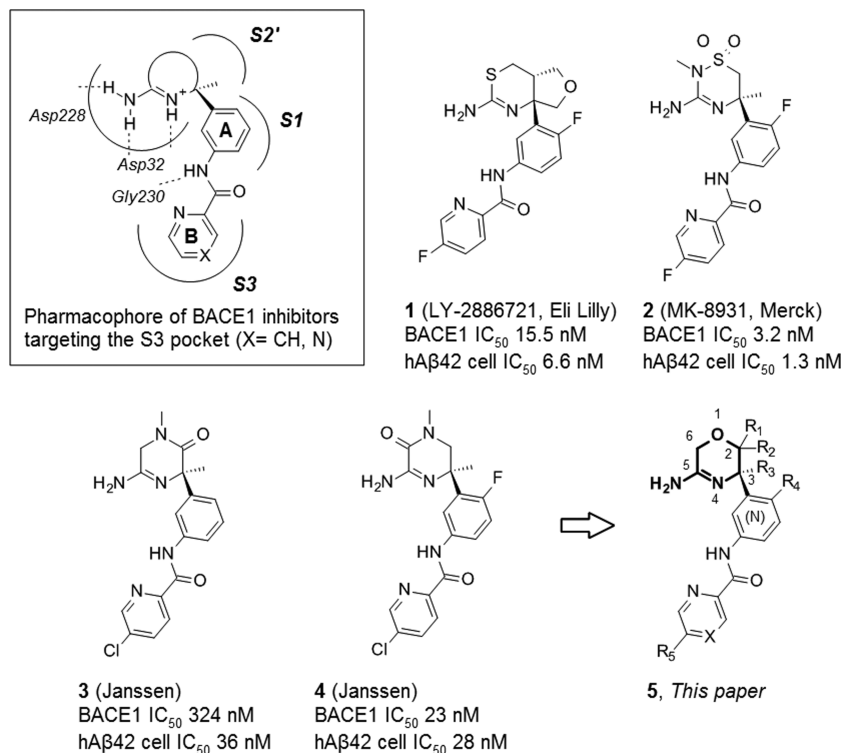
INTRODUCTION

Alzheimer's disease (AD) is a progressive neurodegenerative disorder and the major cause of dementia in the elderly. According to the World Health Organization (WHO), dementia affects 47.5 million people worldwide, a number that is projected to triple by 2050 with the aging population.^{1,2} AD is characterized by progressive deposition of amyloid and misfolded Tau, followed by neurodegeneration and loss of function, leading ultimately to death.³ Of the many attempts to target the underlying pathogenesis, amyloid lowering approaches have made the most progress so far, albeit without delivering a therapy to date.⁴ Amyloid oligomer and plaque formation is thought to occur when the balance between nonamyloidogenic (α -secretase mediated) and the amyloidogenic processing of amyloid precursor protein (APP) is shifted (familial AD) or clearance of amyloid is impaired (sporadic AD).^{5,6} In the amyloidogenic pathway, β -secretase 1 (BACE1) cleaves APP, producing a 99 amino acid length soluble peptide fragment called C99, which is the rate-limiting step in A β formation. This peptide is further processed by γ -secretase to 36–43 amino acid length A β species, of which the longer isoforms, especially A β 42, are the most fibrillogenic and neurotoxic.⁷ Consequently, both β -secretase and γ -secretase are being pursued as targets to

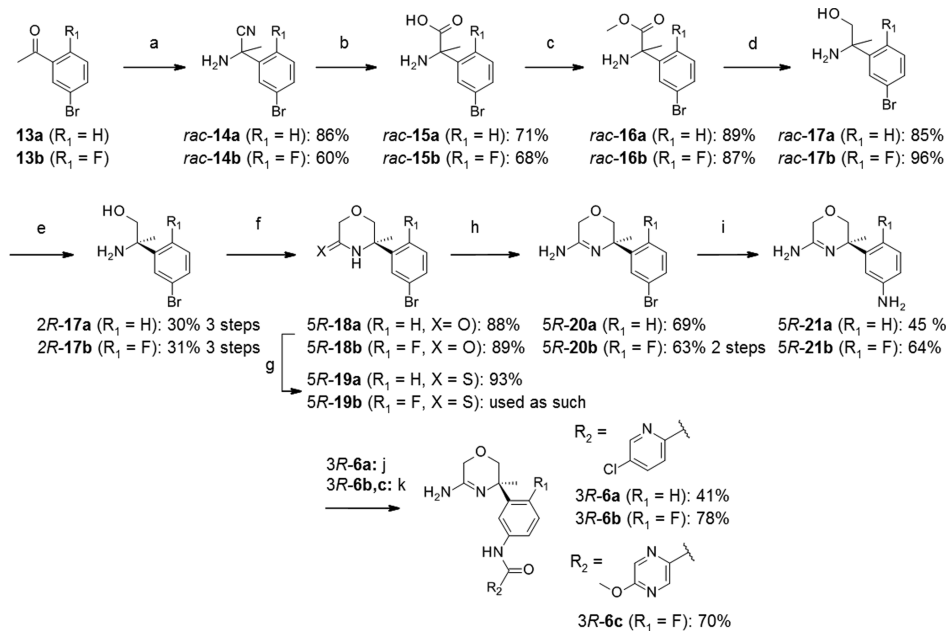
modulate A β production.⁸ Since its discovery in 1999,⁹ BACE1 has been a highly challenging target for drug discovery, and only after years of research medicinal chemists have managed progressing small molecule BACE1 inhibitors in clinical trials.¹⁰ A breakthrough in the development of nonpeptidomimetic BACE1 inhibitors was the identification of amidine- and guanidine-containing small molecules. Compared to previous peptidomimetic and amino-alcohol derived inhibitors, these molecules form a salt bridge and hydrogen bond interactions with Asp32 and Asp228 in the catalytic site of BACE1 in an optimal way (see schematic in Chart 1).¹¹ The use of a quaternary center alpha to the amidine or guanidine function permits substituents to enter adjacent binding pockets such as S2', S1, and S3.¹² The S3 pocket can be efficiently targeted via amide-tethered biaryl systems (Chart 1). In these amidine prototypes, the central aromatic ring (A) is a direct substituent on the quaternary center. The A-ring and amide nitrogen occupy the S1 pocket, whereas the distal aromatic ring (B) extends into the S3 pocket. The B-ring is generally a 2-pyridyl or 2-pyrazinyl ring, allowing for a quasicoplanar orientation with the A-ring.

Received: July 14, 2015

Published: September 17, 2015

Chart 1. Representative Overview of Reported Amidine Containing BACE1 Inhibitors Targeting the S3 Pocket^a

^aInternally generated enzymatic and cellular data are shown.

Scheme 1. Synthesis Route towards 1,4-Oxazines 3R-6a–c^a

^aReagents and conditions: (a) TMSCN, NH₄Cl, 7 N NH₃/MeOH, rt, 4 d; (b) 6 N HCl, reflux, 16 h; (c) H₂SO₄, MeOH, reflux, 16 h; (d) LiAlH₄, THF, 0 °C, 1 h; (e) chiral SFC separation; (f) (i) chloroacetyl chloride, DIPEA, THF, -78 °C, 30 min, (ii) *t*-BuOK, 0 °C, 90 min; (g) P₂S₅, THF, 50 °C, 50 min; (h) 33% NH₃ (aq), 60 °C, 4 h; (i) (i) benzophenone imine, Pd₂(dba)₃, *rac*-BINAP, *t*-BuONa, toluene, 80 °C, 7 h, (ii) 1 N HCl, rt, 16 h; (j) 5-chloropyridine-2-carboxylic acid, HATU, *N,N*-dimethylaniline, DCM, rt, 5 h; (k) 5-methoxypyrazine-2-carboxylic acid, DMTMM, MeOH, rt, 3 h.

The amide NH establishes an interaction with the backbone carbonyl oxygen of Gly230. The fourth substituent on the quaternary center (methyl as shown in the examples in Chart 1) is directed toward the S2' pocket. As such, the field has

progressed toward potent inhibitors with low molecular weight and good ligand efficiency.

A challenge in the development of amidine and guanidine-based BACE1 inhibitors has been to modulate the intrinsic high

basicity of the amidine function. In our previously reported benzoguanidine series,¹³ we found this to be a key factor for obtaining compounds with favorable pharmacokinetic (PK) properties, as high basicity ($pK_a \sim 10-11$) has been associated with unfavorable tissue distribution and P-glycoprotein (P-gp) mediated efflux.¹⁴ Amidine-based warheads with pK_a below 9 have been reported by a number of companies¹⁵ in the form of acyl- and sulfonylguanidines,¹⁶ isoureas,¹⁷ and isothioureas,¹⁸ for which representative examples **1** and **2** are shown in Chart 1.^{19,20} We have previously reported on the de novo design and synthesis of piperazinones **3** and **4** as BACE1 inhibitors with moderate enzymatic and cellular activity.²¹ Interestingly, the amide function embedded in the “warhead” of **3** and **4** helped to decrease the basicity of the amidine, leading to compounds with in vivo activity. However, the blood–brain barrier crossing with this piperazinone series was found to be suboptimal, and concomitantly subcutaneous administration of high doses was needed to achieve significant in vivo reduction of $A\beta$ peptides in mice.

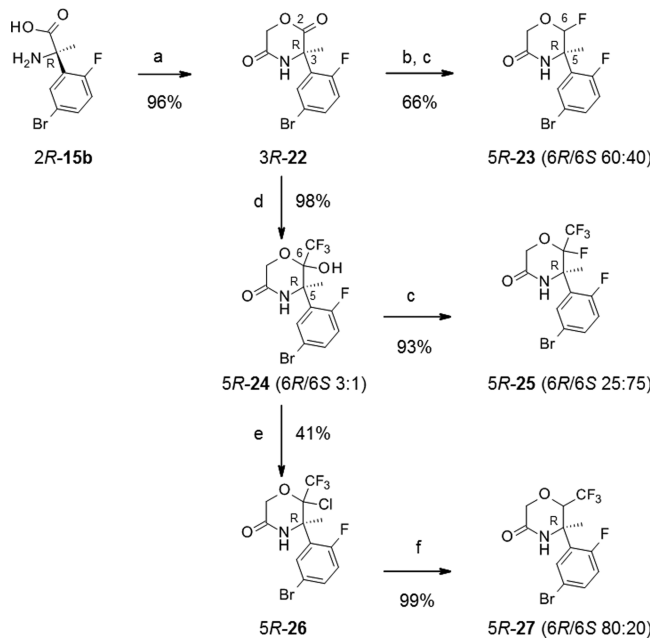
Herein we report the design and synthesis of novel 1,4-oxazines (**5**) as alternative warheads to the previously described piperazinones **3** and **4**. Lead optimization strategies to modify the pK_a of the amidine function resulted in compounds **(2R,3R)-7a** and **(2R,3R)-7d** with a robust oral effect in lowering of $A\beta$ peptides in mouse and dog models.

■ CHEMISTRY

To access 1,4-oxazines **3R-6a–c**, acetophenones **13a,b** were converted to the corresponding amino nitriles **rac-14a,b** via a Strecker reaction (Scheme 1). Acidic hydrolysis of the cyano group and subsequent esterification of the resulting carboxylic acids **rac-15a,b** led to the aminoesters **rac-16a,b**. Reduction of **rac-16a,b** with lithium aluminum hydride (LAH) provided the racemic amino alcohols **rac-17a,b**. Separation of enantiomers via chiral supercritical fluid chromatography (SFC) followed by determination of the absolute stereochemistry by vibrational circular dichroism (VCD) provided the desired enantiomers **2R-17a,b**.²² The lactam rings **5R-18a,b** were constructed next via a one-pot two-step procedure involving amide formation at -15°C in the presence of DIPEA, followed by Williamson etherification with *t*-BuOK. Subsequently, the corresponding amidine derivatives **5R-20a,b** were obtained by sequential thionation of **5R-18a,b** with P_2S_5 , followed by aminolysis of the resulting thioamides **5R-19a,b** with aqueous ammonia. Amination reaction on the bromoarene under Buchwald-type conditions using benzophenone imine as the nitrogen source led to **5R-21a,b**. Finally, the target compounds **3R-6a–c** were obtained via HATU or DMTMM mediated coupling of **5R-21a,b** with the corresponding carboxylic acids.

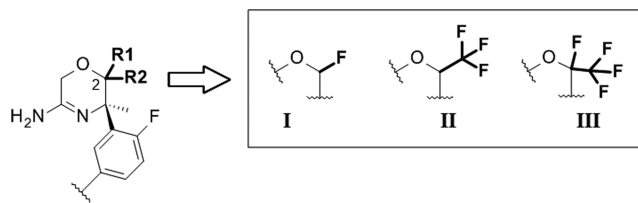
The synthesis routes for target molecules **(2S,3R)-7a**, **(2R,3R)-7a**, **(2S,3R)-8**, **(2R,3R)-8**, **(2R,3R)-9**, and **(2S,3R)-9** bearing electron withdrawing groups (EWG) at the C-2 position start from the common intermediate **2R-15b** (Scheme 2), which was obtained after chiral SFC separation of the racemate **15b** and VCD characterization. Thus, **2R-15b** was cyclized to the morpholine-dione **3R-22** upon reaction with chloroacetyl chloride in a two-step procedure: first the amide bond was formed by treatment with NaOH in 1,4-dioxane, followed by aqueous workup and subsequent lactonization by addition of NaHCO_3 in DMF. Compound **3R-22** proved to be a valuable precursor to access all envisioned modifications (I–III, Chart 2). Reduction of the lactone carbonyl with DIBAL-H to the corresponding hemiacetal, followed by fluorination with

Scheme 2. Synthesis of 1,4-Oxazine-3-one Precursors for BACE1 Targeting Amidines^a



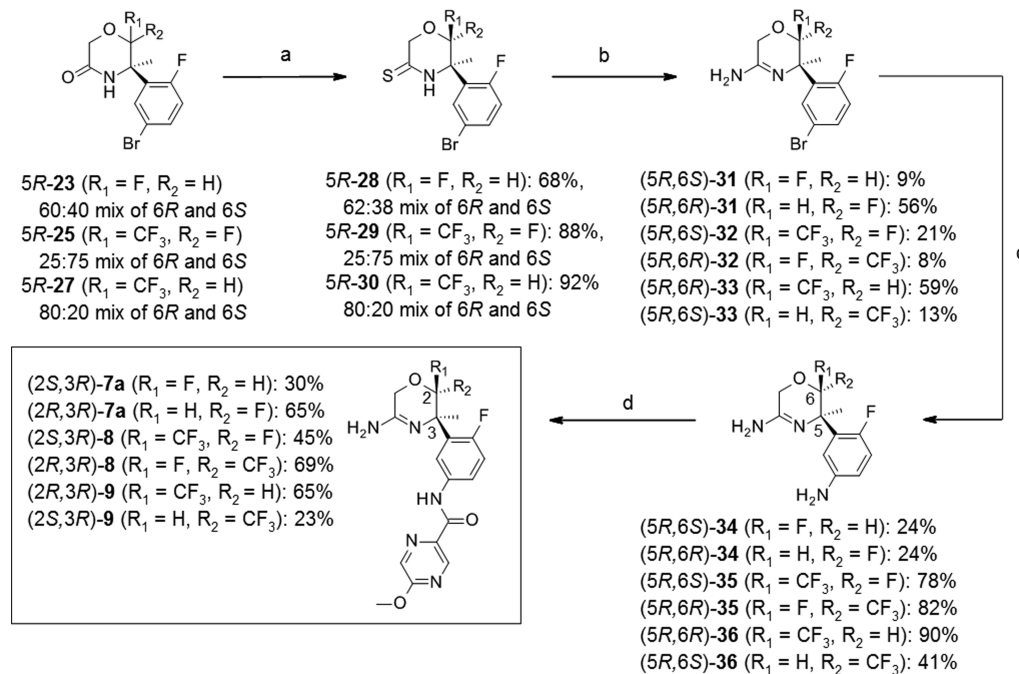
^aReagents and conditions: (a) (i) chloroacetyl chloride, 1 M NaOH, 1,4-dioxane, 2 h, (ii) DMF, NaHCO_3 , 80°C , 3 h; (b) DIBAL-H, THF, -78°C , 2 h; (c) DAST, DCM, 0°C , 40 min (**5R-23**) to 2 h (**5R-25**); (d) TMSCF_3 , TBAT, THF, 0°C to rt, 20 min; (e) SOCl_2 , DCM, 0°C , 30 min, then add pyridine, 0°C , 30 min; (f) Zn, AcOH, 80°C , 3 h.

Chart 2. Scope of Exploration at C-2 Position to Modulate pK_a

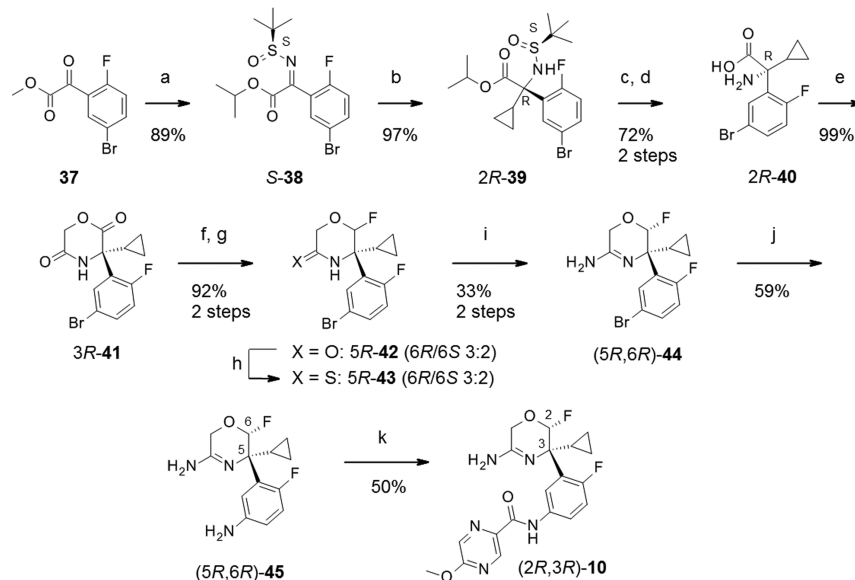


DAST, provided **5R-23** as an inseparable 60:40 mixture of **6R** and **6S** diastereomer. Addition of Ruppert–Prakash reagent (TMSCF_3) to **3R-22** provided hemiketal **5R-24** as an unassigned 3:1 mixture of **6S/6R** diastereomers. Interestingly, **5R-24** also reacted smoothly with DAST, providing the 6-fluoro-6-trifluoromethyl-1,4-oxazine derivatives (**5R,6R)-25** and (**5R,6S)-25** as inseparable mixture in a 25:75 diastereomeric ratio. Hemiketal **5R-24** was also chlorinated by reaction with SOCl_2 , leading to **5R-26**. Treatment of **5R-26** with metallic zinc in acetic acid at 100°C provided the CF_3 derivative **5R-27**, as a 80:20 mixture of **6R** and **6S** diastereomer, respectively.

As shown in Scheme 3, **6R/6S** diastereomeric mixtures **5R-23**, **5R-25**, and **5R-27** were converted to the target amidines (**5R,6S)-31**, (**5R,6R)-31**, (**5R,6S)-32**, (**5R,6R)-32**, (**5R,6R)-33**, and (**5R,6S)-33**) by following a similar reaction sequence to that previously described for **3R-6a–c** in Scheme 1. The only modification in the synthesis route was the conversion of the bromoarene to the aniline, for which we found a copper-catalyzed reaction with sodium azide to provide superior yields to the Buchwald–Hartwig protocol.²³ For occupying the **S3** pocket, the **S-methoxypyrazin-2-yl** group was consistently used to allow for a comparison of properties between the different warheads in

Scheme 3. Preparation of 1,4-Oxazine-Based Amidines C-2 Substituted with Different EWG^a

^aReagents and conditions: (a) P_2S_5 , THF, 70 °C, 2–4 h; (b) 33% NH_3 (aq), 60–80 °C, 24–48 h; (c) NaN_3 , CuI, DMEDA, Na_2CO_3 , DMSO, 110 °C, 1–4 h; (d) 5-methoxypyrazine-2-carboxylic acid, DMTMM, MeOH, 0 °C, 2–6 h.

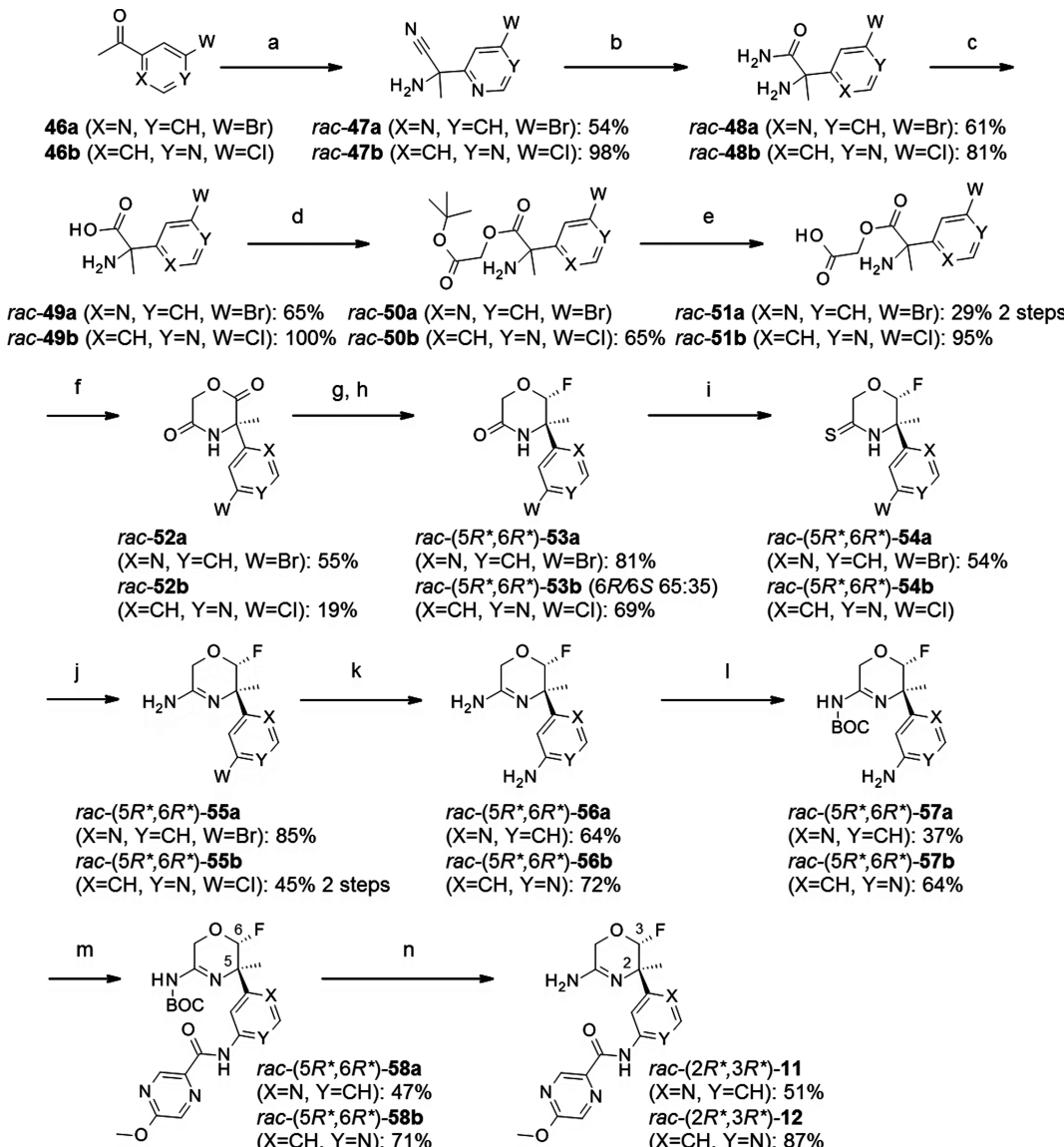
Scheme 4. Enantioselective Synthesis of C-3 Cyclopropyl Substituted 1,4-Oxazine 9^a

^aReagents and conditions: (a) $\text{S}-t\text{BuSONH}_2, \text{Ti}(\text{O}i\text{Pr})_4$, heptane, 80 °C, 24 h; (b) $c\text{PrMgBr}$, DCM, –78 °C, 30 min; (c) 1 M NaOH , MeOH, reflux, 4 h; (d) 4 N HCl in 1,4-dioxane, rt, 1 h; (e) (i) chloroacetyl chloride, 1 M NaOH , 1,4-dioxane, 1 h, (ii) NaHCO_3 , DMF, 80 °C, 2 h; (f) DIBAL-H, THF, –78 °C to rt, 2 h; (g) DAST, DCM, 0 °C, 40 min; (h) P_2S_5 , THF, 70 °C, 4 h; (i) 33% NH_3 (aq), 60 °C, 21 h; (j) NaN_3 , CuI, DMEDA, Na_2CO_3 , DMSO, 110 °C, 1 h; (k) 5-methoxypyrazine-2-carboxylic acid, DMTMM, MeOH, 0 °C, 6 h.

final compounds (2*S*,3*R*)-7*a*, (2*R*,3*R*)-7*a*, (2*S*,3*R*)-8, (2*R*,3*R*)-8, (2*R*,3*R*)-9, and (2*S*,3*R*)-9.

A novel stereoselective route using Ellmann's sulfonamide was developed for the synthesis of compound (2*R*,3*R*)-10 (Scheme 4). Condensation of *S*-Ellmann's sulfonamide with phenylglyoxylic ester (37) in the presence of $\text{Ti}(\text{O}i\text{Pr})_4$ yielded the *S*-sulfoximine S-38. Conveniently, complete transesterification of the methyl ester with 2-propanol occurred during the

condensation step, generating the isopropyl ester, which would be less reactive to the addition of cyclopropyl magnesium bromide in the subsequent reaction step. Similar to the protocol described in ref 22, treatment of S-38 with cyclopropylmagnesium bromide led exclusively to the imine addition product 2*R*-39 with *R*-configuration at the quaternary center. Ester hydrolysis followed by the cleavage of the sulfoxamide S–N bond led to amino acid 3*R*-40, which was next cyclized to the

Scheme 5. Synthesis of 1,4-Oxazines *rac*-(2*R*^{*,3*R*^{*})-11 and *rac*-(2*R*^{*,3*R*^{*})-12 Containing a Pyridyl as A-Ring^a}}

^aReagents and conditions: (a) TMSCN, NH₄Cl, NH₃/MeOH, 12 °C, 4 d; (b) 33% HBr/AcOH, reflux, 12 h; (c) 1 M NaOH, 65 °C, 16 h; (d) ClCH₂CO₂tBu, Cs₂CO₃, DMF, rt, 3 h; (e) TFA, rt, 15 min; (f) 2-chloro-1-methylpyridinium iodide, DIPEA, DCM, reflux, 4 h; (g) DIBAL-H, THF, -78 °C to rt, 90 min; (h) DAST, DCM, 0 °C to rt; (i) P₂S₅, THF, 70 °C, 3 h; (j) 33% NH₃ (aq), 80 °C, 2 h; (k) NaN₃, CuI, DMEDA, Na₂CO₃, DMSO, 110 °C, 24 h; (l) Boc₂O, DCM/ACN 1:1, rt, 22 h; (m) 5-methoxypyrazine-2-carboxylic acid, HATU, DIPEA, DMF, 50 °C, 3 h; (n) TFA, rt, 15 min.

lactone 3*R*-41 following a similar route to the one previously described for 3*R*-22. Reduction of 3*R*-41 with DIBAL-H followed by reaction with DAST provided 5*R*-42 as a 3:2 mixture of 6*R*:6*S* diastereomers. Next, thionation with P₂S₅ to 5*R*-43 and subsequent aminolysis yielded the expected (5*R*,6*R*)-44 after separation of the minor (5*R*,6*S*)-diastereoisomer by column chromatography. Finally, copper-catalyzed coupling of (5*R*,6*R*)-44 with sodium azide to give aniline (5*R*,6*R*)-45, followed by amide formation with 5-methoxypyrazine-2-carboxylic acid, yielded compound (2*R*,3*R*)-10.

Racemic compounds (2*R*^{*,3*R*^{*})-10 and (2*R*^{*,3*R*^{*})-11 were prepared as shown in Scheme 5. First, ketones 46a,b were converted to the α -aminonitriles *rac*-47a,b via a Strecker reaction. Direct acidic hydrolysis of the nitrile group in *rac*-47a,b to the carboxylic acids *rac*-49a,b was not successful in}}

refluxing HCl (aq) due to rapid decarboxylation under the reaction conditions. This could be circumvented by the hydrolysis of the nitriles in *rac*-47a,b to the corresponding amides *rac*-48a,b with HBr in acetic acid, followed by basic hydrolysis with NaOH to *rac*-49a,b. The standard lactonization procedure involving initial *N*-acylation of *rac*-49a,b with chloroacetyl chloride led also to decarboxylation. Fortunately, O-alkylation of *rac*-49a,b with *tert*-butyl chloroacetate to *rac*-50a,b, followed by selective TFA-mediated hydrolysis of the *tert*-butyl ester, yielded the amino acid derivatives *rac*-51a,b. Intramolecular cyclization of *rac*-51a,b with Mukaiyama reagent provided 1,4-oxazine-2,5-diones *rac*-52a,b. A similar reaction sequence to those previously described was used for the transformation of *rac*-52a,b into the target molecules *rac*-(2*R*^{*,3*R*^{*})-11 and *rac*-(2*R*^{*,3*R*^{*})-12. However, because the}}

amidine function in *rac*-(*5R*^{*,}*6R*^{*)-**56a,b** was found to be more reactive toward a peptidic coupling than the aminopyridine fragment using DMTMM, the former needed to be selectively protected with a Boc group, giving *rac*-(*2R*^{*,}*3R*^{*)-**57a,b** prior to coupling reaction with the 5-methoxypyrazine-2-carboxylic acid. Subsequent cleavage of the Boc protecting group in *rac*-(*5R*^{*,}*6R*^{*)-**58a,b** provided *rac*-(*2R*^{*,}*3R*^{*)-**11** and *rac*-(*2R*^{*,}*3R*^{*)-**12**, respectively.}}}}}

■ RESULTS AND DISCUSSION

Our early benzoguanidine series provided us with an understanding of the optimal binding arrangement of the amidine motifs at the catalytic aspartates.¹³ This series suffered from high basicity, examples having measured p*K*_a's in the range of 11 and 12, which we associated with issues of poor permeation, brain penetration, and P-gp efflux. We therefore emphasized the need to find similar amidine and guanidine binding motifs but with reduced basicity, assessed using calculated p*K*_a values. To implicitly capture elements of protein flexibility proposals were docked into multiple BACE1 crystal structures. At this preliminary stage, we were using an entirely in silico approach as previously described.²¹ A similar rational design concept but with different method of execution has been reported by others.²⁴ Alongside the previously reported piperazinones **3** and **4**,²¹ the morpholine series **5** was prioritized highly by our approach. The docking of sample 1,4-oxazine molecules showed them to score particularly well, in fact, they were the best of all ideas profiled and docked optimally into the protein structure PDB 2VA7.¹² With regard to the basicity, the 1,4-oxazine was predicted to be in an ideal range.²⁵ For instance, while our previous benzoguanidines had a calculated basic p*K*_a of 11.1, an oxazine example such as 5-methyl-5-phenyl-5,6-dihydro-2*H*-1,4-oxazin-3-amine had a calculated basic p*K*_a of 6.4 (Scheme 6).²⁵

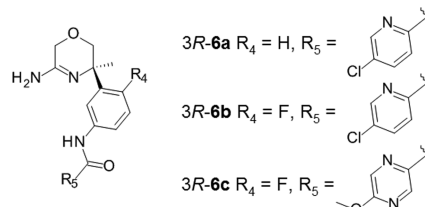
Scheme 6. Comparison of the Calculated p*K*_a To Experiment for Prototype 1,4-Oxazines Using ACD v2014 and AP

p <i>K</i> _a Experiment	9.8	8.1	8.0
p <i>K</i> _a calculated ACD ^a	6.4	3.8	4.6
p <i>K</i> _a calculated ACD ^b	10.4	9.7	9.9
p <i>K</i> _a calculated with AP	9.6	7.3	6.7
Legend	^a Tautomer	^b Tautomer	

This apparently placed the 1,4-oxazines in a good range of basicity, being protonated in the acidic endosome environment in which BACE1 is active and therefore binding at the catalytic aspartates. Such a p*K*_a would be expected to provide a balanced degree of protonation at higher physiological pH, beneficial for CNS drugs.²⁶ However, comparison with the experimental p*K*_a reveals inaccuracy in the calculated value. Deeper analysis of this was performed once more examples were synthesized, and as the later discussion reveals, we may have been fortunate to have prioritized the oxazines via this in silico approach.

The morpholine derivatives **3R-6a–c** were synthesized as early prototypes to set the baseline for potency and physicochemical properties of this class (Table 1). During the course of our

Table 1. In Vitro Profile of Morpholines **3R-6a–c^a**



	3R-6a	3R-6b	3R-6c
BACE1 IC ₅₀ (nM)	44	22	44
hAβ42 cell IC ₅₀ (nM)	9.1	4.1	5.4
mAβ42 cell IC ₅₀ (nM)	7.4	4.5	4.3
hLM (% met @ 15 min)	0	0	1
mLM (% met @ 15 min)	6	10	6
f _u (brain, r, %)	2.9	3.1	10.1
f _u (plasma, h, %)	43	34	56
f _u (plasma, m, %)	28	21	32
P _{app} A > B (nm/s)	nd	38	37
P _{app} A > B + elacridar (nm/s)	nd	231	154
P _{app} ratio	nd	6.0	4.2
p <i>K</i> _a	9.6	9.2	9.0

^aSee Experimental Section for assay details.

research, these molecules were also reported in an extensive warhead exploration published by Hoffmann-La Roche and Siena Biotech.^{19,27} On the basis of previous SAR derived from the exploration of the piperazinone series **4**, 5-chloropyridine-2-carboxamide and 5-methoxy-2-pyrazinecarboxamide were chosen as B-rings to target the S3 pocket in the morpholine probe compounds **3R-6a–c**. In addition, A-ring variations without (**3R-6a**) and with (**3R-6b**) a fluorine atom in *para*-position to the aniline on the A ring (see pharmacophore, Chart 1) were synthesized to assess its influence on p*K*_a and potency. Compounds **3R-6a–c** had satisfactory inhibitory activity in the BACE1 enzymatic assay, with IC₅₀s of 44, 22, and 44 nM, respectively. This potency nicely translated into an inhibition of Aβ42 production of 9.1 nM (**3R-6a**), 4.1 nM (**3R-6b**), and 5.4 nM (**3R-6c**) in a human neuroblastoma cell line. In vivo reduction in Aβ peptides is assessed in mouse, hence determination of the cellular activity of **3R-6a–c** in a mouse neuroblastoma cell line was also done and found to correlate well with the values obtained with the human cell line.

Further profiling of **3R-6a–c** revealed that they had good metabolic stability in human (hLM) and mouse (mLM) liver microsomes, low binding to human and mouse plasma proteins, and moderate nonspecific binding to rat brain homogenate (f_u in plasma or brain). The experimental p*K*_a values were determined for **3R-6a–c** and were found to be higher than predicted (**3R-6a**, 9.6; **3R-6b**, 9.2; **3R-6c**, 9.0). The effect of a fluorine substituent in the A-ring was modest as seen for compound **3R-6b**, which showed only 0.4 Log unit (2.5-fold) reduction in p*K*_a when compared with the nonfluorine substituted analogue **3R-6a**. In line with previous observations that high p*K*_a is associated with increased P-gp efflux,²⁰ high ratios of apparent permeability (P_{app}) in the presence or absence of the P-gp inhibitor elacridar were measured for **3R-6b** and **3R-6c**: 6.0 and 4.2, respectively. Subcutaneous (sc) administration of a 30 mg/kg dose of **3R-6b**

to mouse (Figure 1A) showed modest brain levels (315 ng/g) at 2 h compared to plasma concentration (2397 ng/mL), resulting

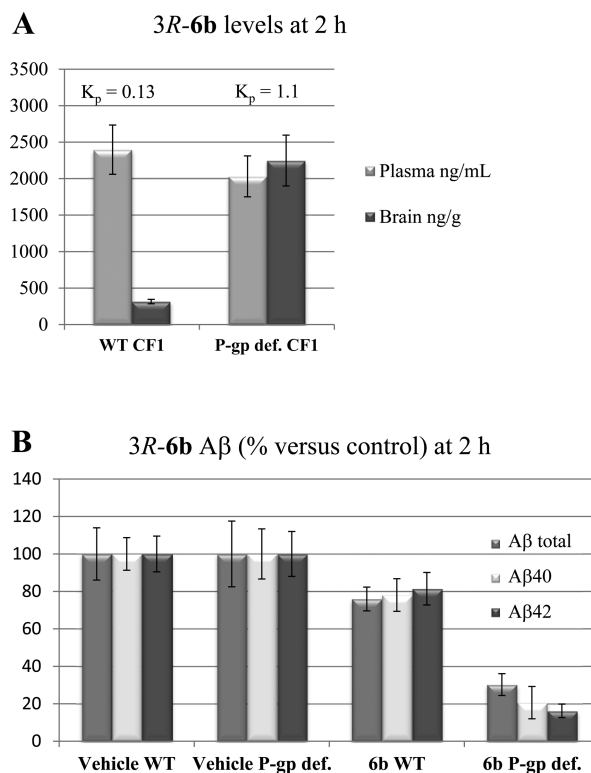


Figure 1. Brain levels (A) and brain A β reduction (B) of 3R-6b in WT and P-gp deficient CF-1 mice (30 mg/kg, sc ($n = 8$); 3R-6b was formulated with 20% SBE β CD at pH 3.5).

in a low brain/plasma ratio (K_p) of 0.13. These low concentrations in the brain translated into a marginal in vivo reduction of A β peptides in the brain of wild-type (WT) CF-1 mice (Figure 1B) 2 h after dosing. When the same experiment was repeated using P-gp deficient CF-1 mice, a more favorable brain/plasma ratio (K_p) of 1.1 was observed, which resulted into a much more pronounced reduction of A β peptides in brain compared to the one observed in WT animals. This experiment confirmed the detrimental role of P-gp efflux in the brain penetration of 3R-6b.

While lower than our old benzoguanidine series, the measured p K_a values were higher than expected from the initial calculations mentioned above.¹³ This prompted a deeper inspection of the accuracy of the calculated p K_a s on these unusual amidine containing ring systems. A selection of 42 compounds containing a cyclic amidine substructure from our compound collection was subjected to experimental p K_a measurement (data in Supporting Information). The selection set encompassed multiple heterocyclic chemotypes and covering approximately a 10 log unit range in calculated p K_a . Molecules with multiple ionizable centers were in general avoided. The p K_a s were calculated with a variety of methods, and the correlation with experiment is shown in Supporting Information. In contrast to previous studies comparing performance across global data sets,²⁸ ADMET predictor performed better than ACD for these amidine ring systems ($R^2 = 0.88$ compared to $R^2 = 0.75$ for best ACD case). This was especially true in the relevant p K_a range of 6–10. These results prompted us to reassess our 1,4-oxazine series with calculations on specific prototypes (Scheme 6), confirming

improved performance when using AP.²⁹ This reiterates the need to calibrate the performance of p K_a calculations for novel chemical systems.

The crystal structure of 3R-6a with BACE1 was solved at 2.6 Å resolution (PDB code 5CLM, Figure 2). The result confirmed a

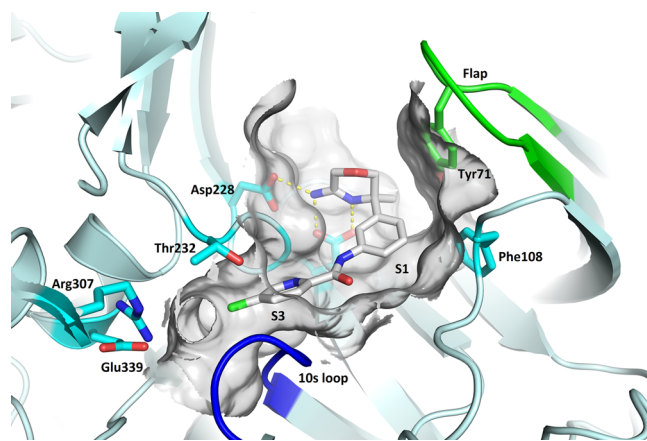


Figure 2. Crystal structure of 3R-6a in BACE1 (1–454). Amino acids as labeled. Active site flap highlighted in green and 10s loop in blue.

binding mode similar to that seen for other bisarylamine substituted amidine BACE1 inhibitors.¹⁷ Namely, the amidine group makes the key and strong network of interactions with the catalytic aspartate dyad (Asp32 and Asp228) involving several hydrogen bonds and a charge–charge interaction between the protonated amidine and anionic acid groups. The A-ring (phenyl) occupies the S1 pocket, and the B-ring (5-chloro-2-pyridyl) enters the S3 pocket. The S1 pocket is formed by amino acids including Phe108, whereas the S3 is bordered by the presence of Thr232 and amino acids from the 10s loop such as Gly11, Gln12, and Gly13 (10s loop, blue in Figure 2). Para substituents on the B-ring approach the salt bridge formed by Arg307 and Glu339. Between the A- and B-ring, the amide N–H forms an H-bond to the backbone carbonyl of Gly230. This bisarylamine has become a widely used group in substituted amidine BACE1 inhibitors, likely because of the optimal shape complementarity with the S1 and S3 pockets.¹⁵

On the basis of the finding that P-gp efflux was influenced by the basicity of the amidine containing warhead, several options for chemical modification of the 1,4-oxazine ring by the introduction of electron withdrawing substituents were possible to reduce its high p K_a . Close inspection of the 1,4-oxazine cycle reveals that the two possible sp³ carbon substitution points have different environments. The carbon which is between the oxygen and the amidine (C-6) is more exposed toward solvent. On the other hand, the carbon between the oxygen and the quaternary carbon (C-2) would direct its substituents toward the active site flap (green in Figure 2). The flap is a well-known feature of the BACE1 binding site; it is flexible and more open at lower pH, correlating with higher enzyme activity.³⁰ It is known to adopt different conformations dependent on the bound inhibitor. Molecules are reported which interact with amino acids such as Tyr71¹³ (Figure 2) and the adjacent Thr72, for example.³⁰ Therefore, given that the amidine warhead was satisfying the interactions at the catalytic aspartates, we set out to target alternative contacts with the flap. Specifically, C-2 position provided an ideal vector to interact with the aromatic ring of

Tyr71, while steric factors would limit the size of the proposed substituents.

An overview of the different modifications explored at C-2 position of the 1,4-oxazine warhead is shown in **Chart 2**. A fluorine (**I**), CF_3 (**II**), and a combination of both groups (**III**) were selected as optimal C-2 substituents to further modulate $\text{p}K_a$ of **3R-6c** while interacting with the active site flap.

BACE1 enzymatic and cellular activity, experimental $\text{p}K_a$ values, P_{app} ratios and Log D values for **3R-6c** and fluorinated 1,4-oxazines (**2S,3R**)-**7a**, (**2R,3R**)-**7a**, (**2S,3R**)-**8**, (**2R,3R**)-**8**, (**2R,3R**)-**9**, and (**2S,3R**)-**9** are provided in **Table 2**.³¹ Interest-

Table 2. Comparison of BACE1 Enzymatic and Cellular Activities, $\text{p}K_a$ s and P_{app} Ratios for Different C-2 Substituted 1,4-Oxazine Warheads^{a,b}

	3R-6c	(2S,3R)- 7a	(2R,3R)- 7a	(2S,3R)- 8	(2R,3R)- 8	(2R,3R)- 9	(2S,3R)- 9
BACE1 IC_{50} (nM)	44	102	12	20	316	29	110
$\text{hAβ42 cell IC}_{50}$ (nM)	5.4	93	9.1	34	324	13	14
P_{app} A>B (nm/s)	37	n. d.	176	n. d.	n. d.	137	n. d.
P_{app} A>B +elacridar (nm/s)	154	n. d.	201	n. d.	n. d.	160	n. d.
P_{app} ratio	4.2	n. d.	1.1	n. d.	n. d.	1.2	n. d.
LogD (pH 7.4)	n. d.	n. d.	2.04	3.43	n. d.	2.52	n. d.
$\text{p}K_a$	9.0	7.6	7.8	6.8	6.9	7.8	8.0

^aSee **Experimental Section** for assay details. ^bn.d.: not determined.

ingly, the 2R-fluoro substituent in (**2R,3R**)-**7a** was found to be highly effective in reducing the basicity of the amidine: a $\text{p}K_a$ of 7.8 was measured, which is a decrease by 1.2 log units when compared with the C-2 nonsubstituted oxazine **3R-6c**. This was aligned with our expectations based on the AP calculated values for this substitution (**Scheme 6**). The reduction in $\text{p}K_a$ was not detrimental for the primary enzymatic and cellular activity, with the discrepancy between both assays decreased when compared to **3R-6c**. This is a general trend observed for our amidine-based BACE1 inhibitors: the lower the $\text{p}K_a$, the smaller the discrepancy becomes between enzymatic and cellular activity. A possible explanation is that highly basic inhibitors accumulate in the acidic endosomes where BACE1 is most active. As such they display apparently higher activity in cellular than biochemical assays, whereas lower $\text{p}K_a$ results in cellular activity in closer accordance with the one in the biochemical assay due to a more uniform distribution of the compound in cellular compartments. Furthermore, compound (**2R,3R**)-**7a** showed good permeability in a LLC-MDR cell line (P_{app} 201 nm/s with elacridar) and a low P_{app} ratio of 1.1, providing additional support to the hypothesis that lowering the amidine $\text{p}K_a$ would have beneficial effects in P_{app} ratios. Interestingly, while in the same $\text{p}K_a$ range, the diastereomeric (**2S,3R**)-**7a** had a much reduced BACE1 IC_{50} of 102 nM, which translated in an equally reduced cellular activity of 93 nM. We hypothesized that this potency difference could be

attributed to the anomeric effect, which favors the 2-fluoro substituent in the axial position. QM calculations indeed confirmed this effect stabilizes the bioactive conformation for (**2R,3R**)-**7a** (see **Supporting Information**). However, in the case of (**2S,3R**)-**7a**, the conformation with the 2-fluorine in axial position places the phenyl in the unfavorable equatorial position for binding to BACE1.³² An additional CF_3 group at C-2 position such as **2S-C(F)CF₃** disubstitution in (**2S,3R**)-**8** reduces $\text{p}K_a$ by another log unit ((**2S,3R**)-**8**, $\text{p}K_a = 6.8$) while maintaining a potency of 20 nM in the BACE1 enzymatic assay. Unfortunately, the **2S-C(F)CF₃** disubstitution had a detrimental effect on the cellular activity and compound (**2S,3R**)-**8** was ~6-fold less potent than **3R-6c**. Interestingly, the diastereoisomeric **2R-C(F)CF₃** 1,4-oxazine (**2R,3R**)-**8** displayed poor inhibitory activity in both enzymatic and cellular assays. This drop in potency could be rationalized after a close inspection of the crystal structure (**Figure 2**) of **3R-6c**, which suggests that the CF_3 group in (**2R,3R**)-**8** would be directed into the face of Tyr71, producing an unfavorable interaction between the negative electrostatic properties of both the CF_3 and the π cloud of Tyr71. A similar but less pronounced trend in enzymatic activity was also observed for the **2-C(H)CF₃** diastereoisomeric pair (**2R,3R**)-**9** ($\text{IC}_{50} = 29$ nM) and (**2S,3R**)-**9** ($\text{IC}_{50} = 110$ nM), although in this case it did not translate in a difference in cellular activity: (**2R,3R**)-**9** $\text{IC}_{50} = 13$ nM vs (**2S,3R**)-**9** $\text{IC}_{50} = 14$ nM. Compound (**2R,3R**)-**9**, with a $\text{p}K_a$ of 7.8, illustrated again the ability of the electron withdrawing ability of the CF_3 group to reduce the amidine $\text{p}K_a$ and its beneficial contribution to a lower P_{app} ratio of 1.2. Similarly, while the permeability for (**2S,3R**)-**8** was not determined, close analogues with different B-rings showed low P_{app} ratios in the 1.2 (5-chloropyridine-2-carboxamide) to 1.6 (4-cyanopyridyl-2-carboxamide) range.

Log D was also measured for the most promising leads (**2R,3R**)-**7a**, (**2S,3R**)-**8**, and (**2R,3R**)-**9**, with (**2R,3R**)-**7a** showing the lowest value (Log $D = 2.04$). From the data obtained, compound (**2R,3R**)-**7a** showed the most balanced profile with good enzymatic and cellular activity, low $\text{p}K_a$ and Log D values and good permeability and P_{app} ratio. Because sugars with anomeric fluorines are known to be hydrolytically unstable,³³ the chemical stability of (**2R,3R**)-**7a** was assessed by LCMS-based experiments under a variety of conditions ranging from acidic to basic media and different temperatures after 7 days (see **Supporting Information**). In these experiments, (**2R,3R**)-**7a** was found to be sufficiently stable at room temperature up to 1 week in buffer at pH 7.4 (92% remaining) and DMSO (100% remaining) to warrant further exploration.

Analysis of the crystal structure of **3R-6a** suggested that space is available around the methyl substituent at the quaternary center in the S2' pocket, hence a limited synthetic effort was devoted to better fill this pocket. Compound (**2R,3R**)-**10** bearing a C-2 fluoro substituent and a cyclopropyl group at position C-3 was selected as a potential target. BACE1 enzymatic and cellular activity, metabolic stability data, and $\text{p}K_a$ values are given for compounds (**2R,3R**)-**10** and (**2R,3R**)-**7a** in **Table 3**. An approximately 5-fold decrease in enzymatic activity was measured for (**2R,3R**)-**10** ($\text{IC}_{50} = 66$ nM) compared to (**2R,3R**)-**7a** ($\text{IC}_{50} = 12$ nM), however, a much more significant 66-fold drop in cellular activity was also observed: (**2R,3R**)-**10** ($\text{IC}_{50} = 603$ nM) vs (**2R,3R**)-**7a** ($\text{IC}_{50} = 9.1$ nM). Compared to (**2R,3R**)-**7a**, (**2R,3R**)-**10** showed increased metabolic stability in hLM but a slightly higher turnover in mLHM. Finally, no difference in $\text{p}K_a$ between (**2R,3R**)-**7a** and (**2R,3R**)-**10** was measured. We

Table 3. Modification on the Quaternary Methyl Group^a

	(2R,3R)-7a	(2R,3R)-10
BACE1 IC ₅₀ nM	12	66
hAβ42 cell IC ₅₀ nM	9.1	603
pK _a	7.8	7.8

^aSee Experimental Section for assay details.

hence decided to maintain the methyl group at the quaternary center for further optimization of (2R,3R)-7a.

To generate additional SAR on potency and pK_a variation of the A-ring was studied next. Analogs *rac*-(2R*,3R*)-11 and *rac*-(2R*,3R*)-12 in which the A-phenyl ring is replaced by a 2- or 4-pyridyl ring were synthesized. BACE1 enzymatic and cellular activity, metabolic stability data, and pK_a values are given for compounds (2R,3R)-7a, *rac*-(2R*,3R*)-11, and *rac*-(2R*,3R*)-12 in Table 4. Interestingly the reduced basicity of

Table 4. Overview of A-Ring Modifications^a

	(2R,3R)-7a	<i>rac</i> -(2R*,3R*)-11	<i>rac</i> -(2R*,3R*)-12
BACE1 IC ₅₀ nM	12	74	3467
hAβ42 cell IC ₅₀ nM	9.1	257	1445
pK _a	7.8	7.8; 2.6	7.6; 2.8

^aSee Experimental Section for assay details.

the amidines was maintained when replacing the phenyl A-ring in (2R,3R)-7a by a 2-pyridyl as in *rac*-(2R*,3R*)-11 (pK_a = 7.8) and the regioisomeric 4-pyridyl analogue *rac*-(2R*,3R*)-12 (pK_a = 7.6). In addition, the pK_a value of the pyridyl nitrogen in *rac*-(2R*,3R*)-11 and *rac*-(2R*,3R*)-12 was measured to be 2.6 and 2.8, respectively, and hence no protonation of this ring is expected to occur under physiological conditions. Unfortunately, while the pK_a of *rac*-(2R*,3R*)-11 and *rac*-(2R*,3R*)-12 was in the desired range, the presence of the pyridyl ring was found to be detrimental for BACE1 activity, with the 2-pyridyl isomer *rac*-(2R*,3R*)-11 significantly less potent than (2R,3R)-7a and *rac*-(2R*,3R*)-12 only active in the μM range.

Finally, a limited SAR exploration of the B-ring in (2R,3R)-7a using different pyridine-2-yl carboxylic acids was performed following a similar synthetic route. A set of representative

compounds (2R,3R)-7a-d along with BACE1 primary activity, data from broader profiling in ADME-tox assays, and physicochemical properties are given in Table 5. Although in

Table 5. Overview of B-Ring Modifications^{a,b}

	(52,63)-7a	(2R,3R)-7b	(2R,3R)-7c	(2R,3R)-7d
BACE1 IC ₅₀ nM	12	7.4	6.9	7.6
hAβ42 cell IC ₅₀ nM	9.1	5.2	3.3	8.1
hLM (% met. @ 15 min)	31	0	16	0
mLM (% met. @ 15 min)	3	17	98	2
dLM (% met. @ 15 min)	70	7	21	0
CYP450 inh. <10 μM	2D6 (0.6)	none	none	2D6 (4.3)
f _u (brain, r, %)	4.4	1.9	1.0	3.9
f _u (plasma, h, %)	60	18	11	41
f _u (plasma, m, %)	28	14	5.0	30
f _u (plasma, d, %)	34	n. d.	n. d.	42
hERG PX (% inh. @ 3 μM)	33	78	52	56
P _{app} A>B (nm/s)	176	85	93	51
P _{app} A>B +elacridar (nm/s)	201	167	142	183
P _{app} ratio	1.1	2.0	1.5	3.6
pK _a	7.8	7.9	7.4	7.9

^aSee Experimental Section for assay details. ^bn.d.: not determined.

general excellent enzymatic and cellular activity data were obtained for all compounds having a pyridyl B-ring ((2R,3R)-7b-d), subtle differences were observed regarding their in vitro ADME properties. For instance, while (2R,3R)-7b and (2R,3R)-7d retained excellent metabolic stability across tested species, the trisubstituted pyridine (2R,3R)-7c was notably unstable in mL. All compounds showed a low potential to inhibit CYP450 isoforms 1A2, 3A4, 2C9, and 2C19 compared to their IC₅₀s. The strongest inhibition of the 2D6 isoform was observed for compound (2R,3R)-7a, with an IC₅₀ of 600 nM, still leading to a 50-fold margin when compared with the enzymatic BACE1 activity (IC₅₀ = 12 nM). In addition, all compounds displayed high free fractions in plasma across species (5.0–60% free) and a reasonable free fraction in rat brain tissue (1.0–4.4% free). Cardiovascular safety of the compounds was first assessed using a hERG channel patch-clamp assay, indicating that the B-ring has a strong effect on hERG inhibition. For instance, while the 5-methoxypyrazine (2R,3R)-7a showed a relatively weak inhibition of the hERG channel at 3 μM (33%), the pyridyl derivative (2R,3R)-7b showed a much stronger hERG inhibition (78%) at the same concentration. This strong interaction could be mitigated by installing a methyl group on the pyridine as in (2R,3R)-7c (52% inhibition). Finally, the 4-cyanopyridyl derivative (2R,3R)-7d showed 56% hERG inhibition at 3 μM. As could be expected for this 2R-F substituted warhead, P_{app} ratios for analogues (2R,3R)-7b-d were generally acceptable, with (2R,3R)-7d being a notable exception with an P_{app} ratio of 3.6.

From the exploration of the B-ring, compounds (2R,3R)-7a and (2R,3R)-7d showed the best balance between potency, hERG liability, and in vitro P-gp efflux liability and therefore were progressed to in vivo PK/PD evaluation. The results obtained are

summarized in Figure 3. In these experiments, compounds were dosed orally (po) to male Swiss mice at 10 mg/kg. Plasma levels

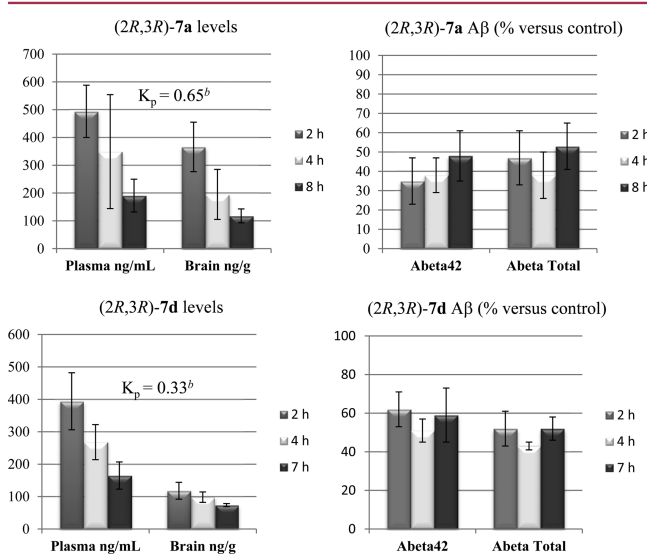


Figure 3. Mouse pharmacokinetic profile of (2R,3R)-7a and (2R,3R)-7d with associated A β levels in brain (10 mg/kg po). Male Swiss SPF mouse fasted ($n = 6$); (2R,3R)-7a formulated with 20% HP β CD at pH 3.9; (2R,3R)-7d formulated with 20% SBE β CD at pH 3.5. (b) Calculated with $AUC_{0-\text{last}}$.

are shown for three time points. For each time point, one hemisphere of the brain was used to conduct bioanalysis and the other hemisphere for AlphaLisa quantification of A β . In line with the measured P_{app} ratios of 1.1 and 3.6, a higher brain uptake relative to plasma was observed for compound (2R,3R)-7a ($K_p = 0.65$) compared to (2R,3R)-7d ($K_p = 0.33$). Gratifyingly, a robust A β 42 reduction of 62% for (2R,3R)-7a and 57% for (2R,3R)-7d was observed in brain homogenate at 4 h after administration, corresponding to brain levels of 195 ng/g for (2R,3R)-7a and 98 ng/g for (2R,3R)-7d. This substantial reduction in A β 42 is in line with their high in vitro potency (respectively 12 and 7.6 nM) and good free fraction in brain. Moreover, this significant reduction of A β 42 in brain is maintained up to 7–8 h.

Because (2R,3R)-7a suffers from a high metabolic turnover in dog liver microsomes (dLM, 70% metabolized after 15 min), the more metabolically stable (2R,3R)-7d was selected for subsequent dog efficacy studies. Dog in vivo plasma concentrations and measured A β levels in cerebrospinal fluid (CSF) after administration of increasing doses from 0.08 to 10 mg/kg are given in Figure 4.³⁴ From this study it can be seen that there is a linear relation between dose and plasma levels with an exceptionally long half-life of about 25 h, which underscores the chemical stability of these fluoromorpholines under physiological conditions. In agreement with this, a dose dependent reduction of A β 42 was observed in CSF, with the 2.5 mg/kg dose showing over 90% reduction of CSF A β 42 up to 50 h post dosing.

CONCLUSIONS

In summary, a novel class of 1,4-oxazine-based BACE1 inhibitors has been identified through rational design. The medicinal chemistry optimization effort through careful structural warhead modification to fine-tune the amidine pK_a along with BACE1 primary activity has resulted in the identification of 2-fluoro-1,4-oxazines (I, Chart 2). Lead optimization efforts identified (2R,3R)-7a and (2R,3R)-7d as potent orally bioavailable BACE1

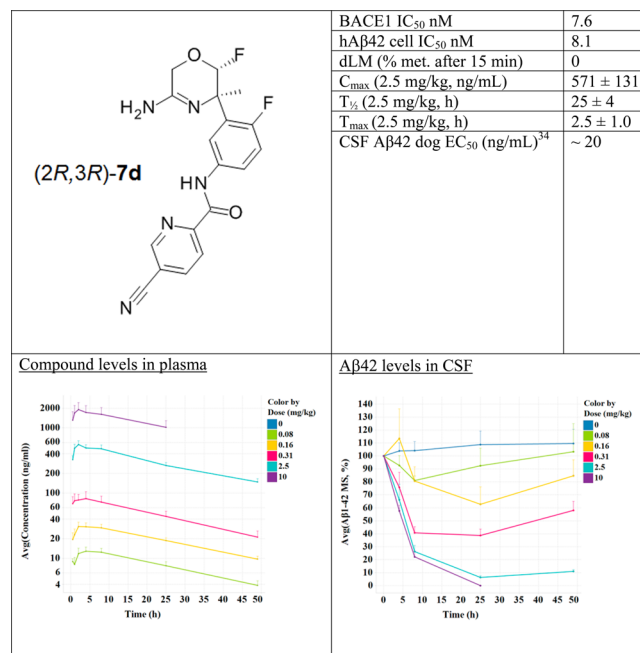


Figure 4. Dog in vivo plasma levels and CSF A β 42 levels of (2R,3R)-7d. Male ($n = 2$ /dose group) and female ($n = 2$ /dose group). Beagle dog fasted; (2R,3R)-7d formulated with 20% HP β CD at pH 3.5.

inhibitors displaying a robust reduction of A β peptides in mice. This amyloid reduction was also confirmed for (2R,3R)-7d in dog, where this compound was able to dose dependently decrease A β levels in CSF up to 50 h post dosing. Challenges remain to navigate the narrow physical chemical property space, especially balancing brain penetration with other critical parameters like metabolic stability and cardiovascular safety (hERG inhibition). Further optimization studies using fluoromorpholines and the other fluorinated warheads described above are under way and will be disclosed in due time.

EXPERIMENTAL SECTION

Enzymatic BACE1 Assay. Primary BACE1 enzymatic activity was assessed by a FRET assay using an amyloid precursor protein (APP) derived 13 amino acids peptide that contains the “Swedish” Lys-Met/Asn-Leu mutation of the APP β -secretase cleavage site as a substrate (Bachem catalogue no. M-2465) and soluble BACE1(1–454) (Aurigene, Custom made). This substrate contains two fluorophores, (7-methoxycoumarin-4-yl) acetic acid (Mca) is a fluorescent donor with excitation wavelength at 320 nm and emission at 405 nm and 2,4-dinitrophenyl (Dnp) is a proprietary quencher acceptor. The increase in fluorescence is linearly related to the rate of proteolysis. In a 384-well format, BACE1 is incubated with the substrate and the inhibitor. The amount of proteolysis is directly measured by fluorescence measurement in the Fluoroskan microplate fluorometer (Thermo scientific). For the low control, no enzyme was added to the reaction mixture.

Cellular A β Assay. Cellular activity was assessed using a SKNBE2 (human) or Neuro-2a (mouse) neuroblastoma cell line expressing the wild-type amyloid precursor protein (hAPP695). The compounds were diluted and added to these cells, incubated for 18 h, and then measurements of A β 42 and A β total were taken. A β 42 and A β total were measured by a sandwich α lisa assay using biotinylated antibody (AbN/25) attached to streptavidin-coated beads and antibody (cAb42/26) conjugated acceptor beads. In the presence of A β 42, the beads come into close proximity. The excitation of the donor beads provokes the release of singlet oxygen molecules that triggers a cascade of energy transfer in the acceptor beads, resulting in light emission.

Metabolic Stability Assay. To test for metabolic stability, compounds (1 μ M) were incubated at 37 °C with mouse, rat, and

human liver microsomes at a protein concentration of 1 mg protein/mL microsomal protein, 1 mM NADPH, 1 mM MgCl₂, and 0.1 M phosphate buffer, pH 7.4. DMSO stock solutions (5 mM) of each compound were diluted with acetonitrile:water (1:1) to provide a working stock solution at 0.1 mM. The total incubation volume was 0.5 mL, with a final total solvent content of 0.01% (v/v) DMSO and 0.5% (v/v) acetonitrile. The reaction was initiated by the addition of 100 μ L prewarmed NADPH solution. The incubation mixture was sampled at 15 min, and the sample quenched with 200 μ L of acetonitrile, centrifuged, and analyzed using a specific HPLC-MS/MS technique. The percentage metabolized was taken as the disappearance of test compound at 15 min.

CYP450 Inhibition Assay. The potential to reversibly inhibit the major human P450 isoforms (CYPs 1A2, 2C9, 2C19, 2D6, and 3A4) was determined using recombinantly expressed human CYPs. Specific probe substrates were used for each CYP isoform which were known to be selectively metabolized to defined fluorescent metabolites. Each test compound was incubated with individual CYPs over a concentration range up to 10 μ M. At the end of the incubation, the level of fluorescence was measured on a plate reader. The level of fluorescence in the presence and absence of test compound was used to determine the IC₅₀ against each CYP isoform.

Plasma Protein Binding Assay. The binding to mouse, dog, and human plasma proteins was determined by rapid equilibrium dialysis (RED device, Thermo Fisher Scientific, Geel, Belgium). The RED device consists of a 48-well plate containing disposable inserts bisected by a semipermeable membrane creating two chambers. A 300 μ L aliquot of plasma containing test compound at 5 μ M was placed on one side and 500 μ L of phosphate buffered saline (PBS) on the other. The plate was sealed and incubated at approximately 37 °C for 4.5 h. After 4.5 h, samples were removed and both the plasma and buffer compartment and analyzed for test compound using a specific HPLC-MS/MS method to estimate free and bound concentrations.

Nonspecific Binding to Brain Tissue Assay. The in vitro nonspecific binding of compounds to rat brain homogenate was determined using the RED device (see above). Each test compound was diluted with rat brain homogenate, prepared following a 1:10 dilution with PBS, to achieve a final concentration of 5 μ M. The plate was incubated at approximately 37 °C for 5 h. After 5 h, samples were removed from both the brain homogenate and buffer compartment and analyzed for test compound using a specific HPLC-MS/MS method to estimate free and bound concentrations.

In Vitro Permeability/P-gp Efflux Assay. The in vitro permeability and potential to be transported by P-glycoprotein (P-gp) was determined using an LLC cell line transfected with human MDR1 (P-glycoprotein). Each test compound (5 μ M) was added to either the apical (A) side of a confluent monolayer of LLC-MDR1 cells and permeability toward the basolateral (B) direction measured by monitoring the appearance of the test compound on the opposite side of the membrane using a specific LC-MS/MS method. Permeability was assessed with and without elacridar (GF 120918, CAS 143851-98-3), a well-known P-gp inhibitor. The A > B+elacridar/A > B ratio (P_{app} ratio) was calculated and used to determine if the test compound was subject to efflux by P-gp.

Mouse in Vivo PK and A β Quantification. Male CD1 Swiss Specific Pathogen Free (SPF) mice (Charles River Company, Germany) were dosed po or sc with the formulated (20% HP β CD) compound. After the indicated time of treatment, the animals were sacrificed and A β levels were analyzed. Blood was collected by decapitation and exsanguinations in EDTA-treated collection tubes. Blood was centrifuged at 1900g for 10 min at 4 °C and the plasma recovered and flash frozen for later analysis. The brain was removed from the cranium and hindbrain. The cerebellum was removed, and the left and right hemisphere were separated. The left hemisphere was stored at -18 °C for quantitative analysis of test compound levels. The right hemisphere was rinsed with phosphate buffered saline (PBS) buffer and immediately frozen on dry ice and stored at -80 °C until homogenization for biochemical assays. The other hemisphere was homogenized and centrifuged and processed for the quantification of A β total and A β 42 via ELISA as described previously.³⁵ Briefly, for the

quantification of A β total A β 42, the antibody pairs JRF/rAb/2 and 4G8 or JRF/cAb42/26 and JRF/rAb/2 antibody were used for capturing and detection, respectively.

Dog in Vivo PK and A β Quantification. Male ($n = 2$ /dose group) and female ($n = 2$ /dose group) beagle dogs were dosed po with the formulated (20% HP β CD) compound or vehicle. At the indicated time points, CSF was sampled in conscious dogs from the lateral ventricle. Quantification of A β 42 in dog CSF was performed using MesoScale Discovery (MSD)'s electrochemiluminescence detection technology as described previously.³⁴

pK_a Assay. Dissociation constants were determined at 25 °C by potentiometric titration of a solution of the compound of interest using a Sirius GlpKa apparatus, and values were calculated using the Henderson-Hasselbach equation. For poorly soluble compounds, titrations were performed with MeOH as cosolvent. In this case pK_a was calculated via Yasuda-Shedlovsky extrapolation.

Log D Assay. The Log D of compounds was determined chromatographically at Sirius Analytical Ltd.³⁶

Analytical Methods. All final compounds were characterized by ¹H NMR and LC/MS. ¹H nuclear magnetic resonance spectra were recorded on Bruker spectrometers: 360 MHz, DPX-400 MHz and AV-500 MHz. Purity of all final compounds was ≥95% by NMR. For the ¹H spectra, all chemical shifts are reported in part per million (δ) units and are relative to the residual signal at 7.26 and 2.50 ppm for CDCl₃ and DMSO, respectively. All the LC/MS analyses were performed using an Agilent G1956A LC/MS quadrupole coupled to an Agilent 1100 series liquid chromatography (LC) system consisting of a binary pump with degasser, autosampler, thermostated column compartment, and diode array detector. The mass spectrometer (MS) was operated with an atmospheric pressure electrospray ionization (API-ES) source in positive ion mode. The capillary voltage was set to 3000 V, the fragmentor voltage to 70 V, and the quadrupole temperature was maintained at 100 °C. The drying gas flow and temperature values were 12.0 L/min and 350 °C, respectively. Nitrogen was used as the nebulizer gas at a pressure of 35 psig. Data acquisition was performed with Agilent Chemstation software. Analyses were carried out on a YMC pack ODS-AQ C18 column (50 mm long × 4.6 mm I.D.; 3 μ m particle size) at 35 °C, with a flow rate of 2.6 mL/min. A gradient elution was performed from 95% (water + 0.1% formic acid)/5% acetonitrile to 5% (water + 0.1% formic acid)/95% acetonitrile in 4.8 min; the resulting composition was held for 1.0 min, from 5% (water + 0.1% formic acid)/95% acetonitrile to 95% (water + 0.1% formic acid)/5% acetonitrile in 0.2 min. The standard injection volume was 2 μ L. Acquisition ranges were set to 190–400 nm for the UV-PDA detector and 100–1400 m/z for the MS detector. Optical rotations measurements were carried out on a 341 PerkinElmer polarimeter in the indicated solvents.

Synthetic Protocols. *N*-(3-[*(3R*)-5-Amino-3-methyl-3,6-dihydro-2*H*-1,4-oxazin-3-yl]phenyl)-5-chloropyridine-2-carboxamide (**3R-6a**). 5-Chloro-2-pyridinecarboxylic acid (0.27 g, 1.72 mmol) was added to a stirred solution of intermediate **5R-21a** (0.235 g, 1.145 mmol) in DCM (10 mL) at rt. Then *N,N*-dimethylaniline (0.218 mL, 1.72 mmol) was added, and after stirring for 5 min at rt, HATU (0.500 g, 1.32 mmol) was added. The mixture was stirred at rt for 5 h. The mixture was diluted with water and satd aq aqueous Na₂CO₃ and extracted with DCM. The organic layer was separated, dried (Na₂SO₄), filtered, and the solvents evaporated in vacuo. The crude product was purified by flash column chromatography (silica; 7 N solution of ammonia in MeOH/DCM 0/100 to 4/96). The desired fractions were collected and concentrated in vacuo. The resulting product was triturated with diisopropyl ether, filtered, and dried. The product was purified again by flash column chromatography (silica; 7 N solution of ammonia in MeOH/EtOAc 0/100 to 4/96). The desired fractions were collected and concentrated in vacuo to yield **3R-6a** (0.16 g, 41% yield). ¹H NMR (500 MHz, CDCl₃) δ 9.85 (br s, 1H), 8.56 (d, *J* = 2.0 Hz, 1H), 8.25 (d, *J* = 8.4 Hz, 1H), 7.88 (dd, *J* = 2.3, 8.4 Hz, 1H), 7.77 (br d, *J* = 8.1 Hz, 1H), 7.71–7.74 (m, 1H), 7.37 (t, *J* = 7.9 Hz, 1H), 7.20 (d, *J* = 7.8 Hz, 1H), 4.25 (br s, 2H), 4.16 (d, *J* = 15.5 Hz, 1H), 4.09 (d, *J* = 15.5 Hz, 1H), 3.74 (d, *J* = 11.4 Hz, 1H), 3.62 (d, *J* = 11.4 Hz, 1H), 1.56 (s, 3H). LC-MS *m/z* 345 [M + H]⁺; $[\alpha]^{20}_{D} = -88.8$ (*c* = 0.68 in DMF).

N-[{(3R)-5-Amino-3-methyl-3,6-dihydro-2H-1,4-oxazin-3-yl]-4-fluorophenyl]-5-chloropyridine-2-carboxamide (3R-6b). 5-Chloro-2-pyridinecarboxylic acid (155 mg, 0.99 mmol) was added to a mixture of 4-(4,6-dimethoxy-1,3,5-triazin-2-yl)-4-methyl morpholinium chloride (297 mg, 1.08 mmol) in MeOH (4 mL). The mixture was stirred for 5 min at rt, after which it was cooled to 0 °C and a solution of aniline 5R-21b in MeOH (4 mL) was added. Then the mixture was stirred at rt for 3 h. The reaction was quenched with half-saturated aq Na₂CO₃ solution and extracted with DCM. The organic layer was separated, dried (Na₂SO₄), filtered, and concentrated in vacuo. The crude product was purified by flash column chromatography (silica; 7 N solution of ammonia in MeOH/DCM 0/100 to 3/97). The desired fractions were collected and the solvents evaporated in vacuo and subsequently triturated with heptane, sonicated, filtered, and dried in vacuo at 50 °C to yield 3R-6b as a white solid (253 mg, 78% yield). ¹H NMR (400 MHz, CDCl₃) δ 9.82 (br s, 1H), 8.54 (d, J = 2.3 Hz, 1H), 8.23 (d, J = 8.3 Hz, 1H), 7.93 (td, J = 3.6, 8.3 Hz, 1H), 7.87 (dd, J = 2.3, 8.5 Hz, 1H), 7.67 (dd, J = 2.8, 6.9 Hz, 1H), 7.05 (dd, J = 8.9, 11.4 Hz, 1H), 4.14 (d, J = 15.3 Hz, 1H), 4.06 (d, J = 15.3 Hz, 1H), 3.92 (dd, J = 0.9, 11.4 Hz, 1H), 3.82 (d, J = 11.4 Hz, 1H), 1.58 (s, 3H) (2H exchanged). ¹³C NMR (101 MHz, DMSO-d₆) δ 161.45, 156.16, 156.36 (d, J = 242.0 Hz, 1C), 148.49, 147.02, 137.80, 134.18, 134.11 (d, J = 14.6 Hz, 1C), 133.80 (br d, J = 2.3 Hz, 1C), 123.80, 122.63 (d, J = 4.6 Hz, 1C), 120.67 (d, J = 8.5 Hz, 1C), 115.70 (d, J = 25.4 Hz, 1C), 70.74 (d, J = 5.8 Hz, 1C), 62.32, 54.70 (d, J = 4.2 Hz, 1C), 26.30 (d, J = 4.2 Hz, 1C). LC-MS m/z 363 [M + H]⁺; [α]²⁰_D = +31.9 (c = 0.69 in DMF); mp = 146.7 °C.

N-[{(3R)-5-Amino-3-methyl-3,6-dihydro-2H-1,4-oxazin-3-yl]-4-fluorophenyl]-5-methoxypyrazine-2-carboxamide (3R-6c). Starting from 5R-19b (100 mg, 0.448 mmol) and following the same procedure as for 3R-6b, the corresponding oxazinamine 3R-6c was obtained (112 mg, 70% yield). ¹H NMR (500 MHz, CDCl₃) δ 9.49 (br s, 1H), 9.00 (d, J = 1.2 Hz, 1H), 8.13 (d, J = 1.2 Hz, 1H), 7.91 (ddd, J = 2.9, 4.0, 8.7 Hz, 1H), 7.64 (dd, J = 2.6, 6.9 Hz, 1H), 7.05 (dd, J = 8.7, 11.6 Hz, 1H), 4.21 (br s, 2H), 4.13 (d, J = 15.5 Hz, 1H), 4.06 (s, 3H), 4.05 (d, J = 15.5 Hz, 1H), 3.92 (dd, J = 1.2, 11.5 Hz, 1H), 3.81 (d, J = 11.5 Hz, 1H), 1.58 (s, 3H). ¹³C NMR (101 MHz, DMSO-d₆) δ 161.61, 161.28, 156.18, 156.30 (d, J = 242.0 Hz, 1C), 142.10, 141.39, 137.95, 133.93 (d, J = 2.7 Hz, 1C), 133.55, 122.69, 120.72 (d, J = 8.1 Hz, 1C), 115.66 (d, J = 25.0 Hz, 1C), 70.76 (d, J = 6.9 Hz, 1C), 62.32, 54.70 (d, J = 3.9 Hz, 1C), 54.26, 26.29 (d, J = 4.2 Hz, 1C). LC-MS m/z 360 [M + H]⁺; [α]²⁰_D = +32.2 (c = 0.61 in DMF); mp = 178.8 °C.

N-[{(2R,3R)-5-Amino-2-fluoro-3-methyl-3,6-dihydro-2H-1,4-oxazin-3-yl]-4-fluorophenyl]-5-methoxypyrazine-2-carboxamide ((2R,3R)-7a). Starting from (5R,6R)-34 (2.42 g, 6.1 mmol) and following the same procedure as for 3R-6b, the corresponding (2R,3R)-7a was obtained as a white solid (1.5 g, 65% yield). ¹H NMR (360 MHz, CDCl₃) δ 9.46 (s, 1H), 8.98 (d, J = 1.5 Hz, 1H), 8.11 (d, J = 1.5 Hz, 1H), 7.83 (ddd, J = 2.7, 4.1, 8.9 Hz, 1H), 7.52 (dd, J = 2.7, 6.8 Hz, 1H), 7.07 (dd, J = 8.8, 11.3 Hz, 1H), 6.04 (d, J = 52.3 Hz, 1H), 4.59 (br s, 2H), 4.26 (d, J = 15.7 Hz, 1H), 4.06 (s, 3H), 4.03 (d, J = 15.7 Hz, 1H), 1.65 (t, J = 2.0 Hz, 3H). ¹³C NMR (101 MHz, DMSO-d₆) δ 161.60, 161.38, 156.16, 155.67 (d, J = 241.4 Hz, 1C), 141.46, 137.91, 134.37 (d, J = 2.2 Hz, 1C), 133.50, 131.61 (dd, J = 5.5, 13.6 Hz, 1C), 121.89 (br d, J = 2.9 Hz, 1C), 121.55 (d, J = 8.8 Hz, 1C), 115.97 (d, J = 25.7 Hz, 1C), 105.00 (dd, J = 7.3, 225.9 Hz, 1C), 57.83 (dd, J = 4.8, 26.8 Hz, 1C), 56.37 (d, J = 2.9 Hz, 1C), 54.24, 25.11 (br d, J = 2.9 Hz, 1C). LC-MS m/z 378 [M + H]⁺; [α]²⁰_D = +117.3 (c = 0.69 in DMF); mp = 212.4 °C.

N-[{(2S,3R)-5-Amino-2-fluoro-3-methyl-morpholin-3-yl]-4-fluorophenyl]-5-methoxypyrazine-2-carboxamide ((2S,3R)-7a). Starting from (5R,6S)-34 (0.040 g, 0.166 mmol) and following the same procedure as for 3R-6b, the corresponding (2S,3R)-7a was obtained (0.019 g, 30%). ¹H NMR (400 MHz, CDCl₃) δ 9.52 (br s, 1H), 9.01 (d, J = 1.3 Hz, 1H), 8.13 (d, J = 1.3 Hz, 1H), 8.03 (ddd, J = 2.9, 4.2, 8.8 Hz, 1H), 7.86 (dd, J = 2.7, 6.7 Hz, 1H), 7.07 (dd, J = 8.8, 11.4 Hz, 1H), 6.09 (dd, J = 1.5, 51.5 Hz, 1H), 4.29 (d, J = 15.6 Hz, 1H), 4.16 (d, J = 15.6 Hz, 1H), 4.06 (s, 3H), 1.55 (s, 3H) (2H exchanged). ¹³C NMR (101 MHz, CDCl₃) δ 162.25, 160.97, 156.59 (d, J = 242.8 Hz, 1C), 153.97, 141.89, 137.35, 133.78 (d, J = 2.2 Hz, 1C), 133.35, 131.25 (d, J = 13.9 Hz, 1C), 120.65 (d, J = 5.1 Hz, 1C), 120.06 (d, J = 8.8 Hz, 1C), 116.28 (d, J = 25.7 Hz, 1C), 105.12 (dd, J = 9.2, 226.3 Hz, 1C), 57.89 (dd, J = 4.4, 25.7 Hz,

1C), 56.18 (d, J = 5.1 Hz, 1C), 54.38, 26.35 (t, J = 4.0 Hz, 1C). LC-MS m/z 378 [M + H]⁺; mp = 211.8 °C.

N-[{(2R,3R)-5-Amino-2-fluoro-3-methyl-3,6-dihydro-2H-1,4-oxazin-3-yl]-4-fluorophenyl]-5-chloropyridine-2-carboxamide ((2R,3R)-7b). Starting from (5R,6R)-34 (500 mg, 2.07 mmol) and following the same procedure as for 3R-6b, the corresponding amide (2R,3R)-7b was obtained as a white solid (600 mg, 76%). ¹H NMR (360 MHz, DMSO-d₆) δ 10.74 (s, 1H), 8.78 (d, J = 2.2 Hz, 1H), 8.19 (dd, J = 2.2, 8.8 Hz, 1H), 8.14 (d, J = 8.8 Hz, 1H), 7.76–7.84 (m, 1H), 7.74 (dd, J = 2.6, 7.3 Hz, 1H), 7.18 (dd, J = 8.8, 11.7 Hz, 1H), 6.07 (br s, 2H), 5.87 (d, J = 53.8 Hz, 1H), 4.04 (d, J = 16.1 Hz, 1H), 3.94 (d, J = 16.1 Hz, 1H), 1.49 (s, 3H). ¹³C NMR (91 MHz, DMSO-d₆) δ 161.61, 156.21, 155.75 (d, J = 241.5 Hz, 1C), 148.51, 147.04, 137.83, 134.30 (d, J = 2.1 Hz, 1C), 134.23, 131.67 (dd, J = 5.5, 13.8 Hz, 1C), 123.93, 121.98, 121.60 (d, J = 8.3 Hz, 1C), 116.05 (d, J = 25.6 Hz, 1C), 105.01 (dd, J = 6.9, 226.3 Hz, 1C), 57.85 (dd, J = 4.5, 26.6 Hz, 1C), 56.39 (d, J = 3.5 Hz, 1C), 25.15 (br d, J = 5.5 Hz, 1C). LC-MS m/z 381 [M + H]⁺; mp = 220.4 °C.

N-[{(2R,3R)-5-Amino-2-fluoro-3-methyl-3,6-dihydro-2H-1,4-oxazin-3-yl]-4-fluorophenyl]-5-chloropyridine-2-carboxamide Hydrochloride ((2R,3R)-7c). Starting from (5R,6R)-34 (150 mg, 0.38 mmol) and following the same procedure as for 3R-6b, the corresponding amide (2R,3R)-7c was obtained. The purified compound (2R,3R)-7c was dissolved in 2-propanol/DIPE, and a few drops of a 6 N HCl solution in 2-propanol were added. The resulting precipitate was collected after evaporation of the solvents, yielding (2R,3R)-7c as a white solid (77 mg, 47%, HCl salt). ¹H NMR (360 MHz, DMSO-d₆) δ 11.18 (s, 1H), 10.80 (s, 1H), 9.68 (s, 1H), 8.98 (s, 1H), 8.60 (d, J = 2.6 Hz, 1H), 8.05–8.07 (m, 1H), 8.01 (ddd, J = 2.6, 4.2, 9.0 Hz, 1H), 7.75 (dd, J = 2.6, 7.3 Hz, 1H), 7.33 (dd, J = 9.0, 11.9 Hz, 1H), 6.15 (d, J = 50.5 Hz, 1H), 4.76 (d, J = 17.9 Hz, 1H), 4.67 (d, J = 17.9 Hz, 1H), 2.58 (s, 3H), 1.73 (s, 3H). ¹³C NMR (101 MHz, DMSO-d₆) δ 163.98, 162.16, 154.88 (d, J = 243.1 Hz, 1C), 147.75, 144.36, 139.66, 135.82, 135.45 (d, J = 2.3 Hz, 1C), 132.70, 126.52 (dd, J = 4.2, 12.3 Hz, 1C), 122.23 (d, J = 8.5 Hz, 1C), 119.63, 117.12 (d, J = 24.7 Hz, 1C), 104.28 (dd, J = 5.8, 232.7 Hz, 1C), 58.19 (dd, J = 4.2, 25.4 Hz, 1C), 56.99 (d, J = 4.2 Hz, 1C), 21.71 (dd, J = 2.5, 4.8 Hz, 1C), 18.88. LC-MS m/z 395 [M + H]⁺; mp = 129.4 °C.

N-[{(2R,3R)-5-Amino-2-fluoro-3-methyl-3,6-dihydro-2H-1,4-oxazin-3-yl]-4-fluorophenyl]-5-cyanopyridine-2-carboxamide ((2R,3R)-7d). Starting from (5R,6R)-34 (834 mg, 3.46 mmol) and following the same procedure as for 3R-6b, the corresponding amide (2R,3R)-7d was obtained as a white solid (615 mg, 48%). ¹H NMR (500 MHz, DMSO-d₆) δ 10.86 (s, 1H), 9.19 (d, J = 2.0 Hz, 1H), 8.57 (dd, J = 2.0, 8.1 Hz, 1H), 8.27 (d, J = 8.1 Hz, 1H), 7.78–7.83 (m, 1H), 7.76 (dd, J = 2.6, 7.2 Hz, 1H), 7.18 (dd, J = 8.7, 11.8 Hz, 1H), 6.05 (br s, 2H), 5.87 (d, J = 53.7 Hz, 1H), 4.04 (d, J = 15.9 Hz, 1H), 3.94 (d, J = 15.9 Hz, 1H), 1.49 (s, 3H). ¹³C NMR (101 MHz, DMSO-d₆) δ 161.17, 156.21, 155.87 (d, J = 242.1 Hz, 1C), 152.54, 151.42, 142.10, 134.08 (d, J = 2.2 Hz, 1C), 131.70 (dd, J = 5.9, 13.2 Hz, 1C), 122.34, 122.08 (br d, J = 2.2 Hz, 1C), 121.74 (d, J = 8.8 Hz, 1C), 116.55, 116.06 (d, J = 25.7 Hz, 1C), 111.48, 104.98 (dd, J = 7.3, 225.9 Hz, 1C), 57.84 (dd, J = 4.8, 26.8 Hz, 1C), 56.38 (d, J = 3.7 Hz, 1C), 25.09 (br d, J = 3.7 Hz, 1C). LC-MS m/z 372 [M + H]⁺; [α]²⁰_D = +125.0 (c = 0.51 in DMF); mp = 223.4 °C.

N-[{(2S,3R)-5-Amino-2-fluoro-3-methyl-2-(trifluoromethyl)-3,6-dihydro-2H-1,4-oxazin-3-yl]-4-fluorophenyl]-5-methoxypyrazine-2-carboxamide ((2S,3R)-8). Starting from (5R,6S)-35 (0.20 g, 0.65 mmol) and following the same procedure as for 3R-6b, the corresponding (2S,3R)-8 was obtained as a white solid (0.13 g, 45% yield). ¹H NMR (360 MHz, CDCl₃) δ 9.49 (br s, 1H), 9.02 (d, J = 1.3 Hz, 1H), 8.16 (d, J = 1.3 Hz, 1H), 7.84 (dd, J = 2.9, 7.3 Hz, 1H), 7.64 (td, J = 3.3, 8.8 Hz, 1H), 7.02 (dd, J = 8.8, 12.4 Hz, 1H), 4.44–4.56 (m, 2H), 4.34 (br s, 2H), 4.07 (s, 3H), 1.87 (br s, 3H). ¹³C NMR (101 MHz, DMSO-d₆) δ 161.62, 161.56, 157.33 (d, J = 245.8 Hz, 1C), 154.03, 141.57, 137.96, 134.14 (d, J = 2.2 Hz, 1C), 133.46, 127.24 (dd, J = 4.8, 10.6 Hz, 1C), 122.75 (d, J = 1.5 Hz, 1C), 121.92 (d, J = 9.5 Hz, 1C), 120.65 (dq, J = 35.2, 286.8 Hz, 1C), 116.16 (d, J = 26.4 Hz, 1C), 106.52 (qd, J = 32.3, 240.6 Hz, 1C), 59.02, 58.41 (br d, J = 30.1 Hz, 1C), 54.26, 25.17. LC-MS m/z 444 [M - H]⁻; [α]²⁰_D = +75.6 (c = 0.17 in MeOH); mp = 80.0 °C.

N-[{(2R,3R)-5-Amino-2-fluoro-3-methyl-2-(trifluoromethyl)-3,6-dihydro-2H-1,4-oxazin-3-yl]-4-fluorophenyl]-5-methoxypyrazine-2-carboxamide ((2R,3R)-8). Starting from (5R,6R)-35 (0.2 g, 0.65 mmol)

and following the same procedure as for **3R-6b**, the corresponding (*2R,3R*)-**8** was obtained (200 mg, 69% yield). ¹H NMR (360 MHz, CDCl₃) δ 9.49 (br s, 1H), 9.02 (d, J = 1.5 Hz, 1H), 8.15 (d, J = 1.5 Hz, 1H), 7.83–7.89 (m, 1H), 7.67 (td, J = 2.4, 6.9 Hz, 1H), 7.04 (dd, J = 8.8, 12.1 Hz, 1H), 4.53 (d, J = 15.7 Hz, 1H), 4.46 (d, J = 15.7 Hz, 1H), 4.38 (br s, 2H), 4.07 (s, 3H), 1.83 (s, 3H). ¹³C NMR (101 MHz, DMSO-*d*₆) δ 161.60, 161.38, 157.26 (d, J = 245.8 Hz, 1C), 153.70, 141.43, 137.97, 133.56 (d, J = 2.2 Hz, 1C), 133.47, 128.28 (d, J = 11.0 Hz, 1C), 125.27, 121.76 (d, J = 8.8 Hz, 1C), 121.00 (dq, J = 35.2, 289.8 Hz, 1C), 115.55 (d, J = 27.1 Hz, 1C), 106.34 (qd, J = 33.8, 204.7 Hz, 1C), 59.07 (d, J = 2.9 Hz, 1C), 58.42 (dd, J = 2.9, 25.7 Hz, 1C), 54.24, 24.13 (br d, J = 6.6 Hz, 1C). LC-MS *m/z* 444 [M + H]⁺; [a]_D²⁰ = -128.6 (c = 0.22 in MeOH); mp = 198.4 °C.

N-{[*(2R,3R*)-5-Amino-3-methyl-2-(trifluoromethyl)-3,6-dihydro-2*H*-1,4-oxazin-3-yl]-4-fluorophenyl}-5-methoxypyrazine-2-carboxamide (*(2R,3R*)-**9**). Starting from (*5R,6R*)-**36** (0.20 g, 0.69 mmol) and following the same procedure as for **3R-6b**, the corresponding (*2R,3R*)-**9** was obtained (0.19 g, 65% yield). ¹H NMR (360 MHz, CDCl₃) δ 9.55 (br s, 1H), 9.02 (d, J = 1.5 Hz, 1H), 8.15 (d, J = 1.5 Hz, 1H), 8.02 (ddd, J = 2.9, 4.4, 8.8 Hz, 1H), 7.89 (dd, J = 2.7, 6.8 Hz, 1H), 7.05 (dd, J = 8.8, 11.7 Hz, 1H), 4.65 (q, J = 8.2 Hz, 1H), 4.32 (br s, 2H), 4.23 (s, 2H), 4.07 (s, 3H), 1.68 (s, 3H). ¹³C NMR (91 MHz, DMSO-*d*₆) δ 161.66, 161.35, 156.95 (d, J = 243.0 Hz, 1C), 155.06, 141.43, 137.97, 133.97 (d, J = 2.1 Hz, 1C), 133.59, 130.44 (d, J = 13.1 Hz, 1C), 122.70 (d, J = 3.5 Hz, 1C), 121.22 (d, J = 9.0 Hz, 1C), 124.33 (q, J = 286.5 Hz, 1C), 115.39 (d, J = 24.9 Hz, 1C), 73.25 (q, J = 26.3 Hz, 1C), 59.45, 54.78 (d, J = 3.5 Hz, 1C), 54.30, 28.57 (d, J = 2.8 Hz, 1C). LC-MS *m/z* 428 [M + H]⁺; [a]_D²⁰ = -42.4 (c = 0.18 in MeOH); mp = 252.5 °C.

N-{[*(2S,3R*)-5-Amino-3-methyl-2-(trifluoromethyl)-3,6-dihydro-2*H*-1,4-oxazin-3-yl]-4-fluorophenyl}-5-methoxypyrazine-2-carboxamide (*(2S,3R*)-**9**). Starting from (*5R,6S*)-**36** (0.10 g, 0.34 mmol) and following the same procedure as for **3R-6b**, the corresponding (*2S,3R*)-**9** was obtained (0.034 g, 23% yield). ¹H NMR (400 MHz, DMSO-*d*₆) δ 10.44 (br s, 1H), 8.88 (d, J = 1.3 Hz, 1H), 8.38 (d, J = 1.3 Hz, 1H), 7.94 (dd, J = 2.6, 7.5 Hz, 1H), 7.84–7.91 (m, 1H), 7.11 (dd, J = 8.8, 12.1 Hz, 1H), 5.76 (br s, 2H), 4.41 (q, J = 7.6 Hz, 1H), 4.26 (d, J = 15.5 Hz, 1H), 4.20 (d, J = 15.5 Hz, 1H), 4.01 (s, 3H), 1.56 (s, 3H). ¹³C NMR (101 MHz, DMSO-*d*₆) δ 161.63, 161.44, 156.66 (d, J = 243.6 Hz, 1C), 154.73, 141.50, 137.91, 134.26 (d, J = 2.2 Hz, 1C), 133.47, 132.04 (d, J = 10.3 Hz, 1C), 121.29 (d, J = 3.7 Hz, 1C), 120.82 (d, J = 8.8 Hz, 1C), 124.16 (q, J = 283.9 Hz, 1C), 115.99 (d, J = 24.9 Hz, 1C), 74.63 (dq, J = 5.1, 27.9 Hz, 1C), 62.50, 55.57 (d, J = 3.7 Hz, 1C), 54.26, 22.23. LC-MS *m/z* 428 [M + H]⁺; mp = 214.7 °C.

N-{[*(2R,3R*)-5-Amino-3-cyclopropyl-2-fluoro-2,6-dihydro-1,4-oxazin-3-yl]-4-fluorophenyl}-5-methoxy-pyrazine-2-carboxamide (*(2R,3R*)-**10**). Starting from (*5R,6R*)-**45** (0.20 g, 0.75 mmol) and following the same procedure as for **3R-6b**, the corresponding (*2R,3R*)-**10** was obtained (0.15 g, 50% yield). ¹H NMR (360 MHz, CDCl₃) δ 9.46 (s, 1H), 8.99 (d, J = 1.5 Hz, 1H), 8.13 (d, J = 1.46 Hz, 1H), 7.82 (ddd, J = 2.93, 4.03, 8.78 Hz, 1H), 7.39 (dd, J = 2.74, 6.77 Hz, 1H), 7.08 (dd, J = 8.78, 11.71 Hz, 1H), 6.22 (d, J = 52.33 Hz, 1H), 4.44 (br s, 2H), 4.22 (d, J = 15.37 Hz, 1H), 4.06 (s, 3H), 3.99 (d, J = 15.37 Hz, 1H), 1.65 (dt, J = 3.29, 8.42 Hz, 1H), 0.50–0.60 (m, 1H), 0.47 (d, J = 15.00 Hz, 1H), 0.38 (qd, J = 4.88, 9.51 Hz, 1H), 0.17–0.26 (m, 1H). ¹³C NMR (101 MHz, DMSO-*d*₆) δ 161.57 (br d, J = 5.1 Hz, 1C), 161.35, 157.37, 155.70 (d, J = 240.6 Hz, 1C), 141.45, 137.93, 134.24 (d, J = 2.2 Hz, 1C), 133.50, 131.79 (br d, J = 12.5 Hz, 1C), 121.92 (d, J = 3.7 Hz, 1C), 121.36 (d, J = 8.8 Hz, 1C), 115.90 (d, J = 25.7 Hz, 1C), 105.37 (dd, J = 8.4, 226.3 Hz, 1C), 58.75 (dd, J = 5.1, 27.9 Hz, 1C), 56.95 (d, J = 2.9 Hz, 1C), 54.24, 16.02 (d, J = 6.6 Hz, 1C), 2.20, -1.60. LC-MS *m/z* 404 [M + H]⁺.

rac-N-{[*(2R*,3R*)-5-Amino-2-fluoro-3-methyl-3,6-dihydro-2H-1,4-oxazin-3-yl]pyridin-4-yl]-5-methoxypyrazine-2-carboxamide (*rac-(2R*,3R*)-11*). Di-tert-butyl dicarbonate (0.85 g, 3.88 mmol) was added to 0.54 g (2.43 mmol) of aniline *rac*-(*5R*,6R**)-**56a** in 100 mL of DCM/ACN (1:1), and the resulting mixture was stirred 22 h at rt. Then, all volatiles were evaporated at rt and the crude was purified by flash column chromatography (silica; 7 N solution of NH₃ in MeOH/DCM 0/100 to 10/90). The product fractions were evaporated, providing the Boc-amidine *rac*-(*5R*,6R**)-**57a** as a yellow oil (0.29 mg, 37% yield), and another fraction of starting material *rac*-(*5R*,6R**)-**56a** was recovered (0.27 g, 49%).*

HATU (0.18 g, 0.46 mg) was added to a solution of *rac*-(*5R*,6R**)-**57a** (0.050 g, 0.154 mmol), 5-methoxypyrazine-2-carboxylic acid (0.071 g, 0.462 mmol), and DIPEA (0.16 mL, 0.925 mmol) in 2 mL of dry DMF, and the resulting mixture was stirred 3 h at 50 °C. After cooling to rt, DCM and 2 N Na₂CO₃ were added to the mixture and it was stirred for 30 min at rt. The organic layer was separated and the aqueous layer was extracted with DCM. The combined organic layers were dried (Na₂SO₄), filtered, and concentrated. The residue was purified by flash column chromatography (silica; 7 N solution of ammonia in MeOH/DCM 0/100 to 10/90). The desired fractions were collected and concentrated in vacuo, yielding amide *rac*-(*5R*,6R**)-**58** as a transparent oil (33.1 mg, 47%).

rac-(*5R*,6R**)-**58a** (33.1 mg, 0.0719 mmol) was dissolved in TFA (3 mL) and stirred for 15 min. Then, the mixture was evaporated to dryness and satd aq NaHCO₃ and DCM were added. The biphasic mixture was stirred until gas evolution ceased, and then the organic layer was separated. The aqueous layer was extracted twice with DCM. The combined organic layers were dried (Na₂SO₄), filtered, and the solvent was evaporated. The residue was purified by flash column chromatography (silica; 7 N solution of ammonia in MeOH/DCM 0/100 to 10/90). The desired fractions were collected and concentrated in vacuo, yielding *rac*-(*2R*,3R**)-**11** as beige crystals, which were washed with diethyl ether and dried in vacuo at 50 °C (14.8 mg, 51%). ¹H NMR (360 MHz, DMSO-*d*₆) δ 10.89 (br s, 1H), 8.92 (d, J = 1.3 Hz, 1H), 8.44 (d, J = 5.7 Hz, 1H), 8.43 (d, J = 1.3 Hz, 1H), 7.96 (d, J = 1.9 Hz, 1H), 7.75 (dd, J = 1.9, 5.7 Hz, 1H), 6.02 (br s, 2H), 5.92 (d, J = 54.5 Hz, 1H), 4.06 (d, J = 16.1 Hz, 1H), 4.03 (s, 3H), 3.95 (d, J = 16.1 Hz, 1H), 1.42 (d, J = 0.7 Hz, 3H). ¹³C NMR (101 MHz, DMSO-*d*₆) δ 164.99, 162.49, 161.81, 156.02, 149.08, 145.79, 142.01, 137.49, 133.63, 112.39, 111.55 (d, J = 1.9 Hz, 1C), 107.06 (d, J = 225.4 Hz, 1C), 60.40 (d, J = 25.4 Hz, 1C), 56.41 (d, J = 3.9 Hz, 1C), 54.36, 26.02. LC-MS *m/z* 361 [M + H]⁺; mp, decomposition around 230 °C.

rac-N-{[*(2R*,3R*)-5-Amino-2-fluoro-3-methyl-3,6-dihydro-2H-1,4-oxazin-3-yl]pyridin-2-yl]-5-methoxypyrazine-2-carboxamide (*rac-(2R*,3R*)-12*). Di-tert-butyl dicarbonate (0.234 g, 1.07 mmol) was added portionwise to a stirred solution of intermediate *rac*-(*5R*,6R**)-**56b** (0.200 g, 0.892 mmol), triethylamine (1.00 mL, 19.1 mmol), and 4-dimethylaminopyridine (0.006 g, 0.05 mmol) in THF (1 mL) at rt for 3 h. The mixture was quenched with satd aq NaHCO₃ solution. The aqueous layer was extracted with EtOAc. The organic layer was dried (MgSO₄), filtered, and the solvents evaporated in vacuo to yield the corresponding Boc-amidine *rac*-(*5R*,6R**)-**57b** (0.185 g, 64% yield), which was used as such in the then reaction step.*

HATU (70.3 mg, 0.185 mmol) was added to a solution of *rac*-(*5R*,6R**)-**57b** (50.0 mg, 0.154 mmol), 5-methoxypyrazine-2-carboxylic acid (28.5 mg, 0.185 mmol), and DIPEA (79.7 mL, 0.462 mmol) in dry DMF (2 mL), and the resulting mixture was stirred overnight at rt. The solvent was evaporated, and the residue was taken up in DCM and 2 N Na₂CO₃. The organic layer was separated, and the aqueous layer was extracted with DCM. The combined organic layers were dried (Na₂SO₄), filtered, and concentrated. The residue was purified by flash column chromatography (silica; 7 N solution of ammonia in MeOH/DCM 0/100 to 10/90). The desired fractions were collected and concentrated in vacuo yielding providing *rac*-(*5R*,6R**)-**58b** as a transparent glass (50.5 mg, 71%).

rac-(*5R*,6R**)-**58b** (50 mg) was dissolved in TFA (5 mL), and the resulting mixture was stirred for 15 min before it was evaporated to dryness. Satd aq NaHCO₃ and DCM were added, the biphasic mixture was stirred until gas evolution ceased, and then the organic layer was separated. The aqueous layer was extracted twice with DCM. The combined organic layers were separated, dried (MgSO₄), and the solvent was evaporated, providing *rac*-(*2R*,3R**)-**12** as off-white crystals, which were triturated with diethyl ether, filtered, and dried in vacuo at 50 °C (34.2 mg, 87%). ¹H NMR (360 MHz, DMSO-*d*₆) δ 10.06 (s, 1H), 8.95 (d, J = 1.2 Hz, 1H), 8.45 (d, J = 1.2 Hz, 1H), 8.32 (d, J = 5.3 Hz, 1H), 8.28 (d, J = 1.6 Hz, 1H), 7.24 (dd, J = 1.6, 5.3 Hz, 1H), 6.13 (br s, 2H), 5.82 (br d, J = 52.7 Hz, 1H), 4.10 (d, J = 15.4 Hz, 1H), 4.03 (s, 3H), 4.00 (d, J = 15.4 Hz, 1H), 1.45 (d, J = 0.7 Hz, 3H). ¹³C NMR (101 MHz, DMSO-*d*₆) δ 162.05, 161.06, 156.45 (br s, 2C), 150.88, 148.06, 141.55, 136.66, 134.04, 118.02, 111.18, 106.36 (d, J = 227.3 Hz, 1C),

58.49 (d, $J = 25.8$ Hz, 1C), 56.69 (d, $J = 3.9$ Hz, 1C), 54.44, 25.69. LC-MS m/z 361 [M + H]⁺.

rac-2-Amino-2-(3-bromophenyl)-propionitrile (*rac*-14a**).** Trimesylsilyl cyanide (20 g, 200 mmol) was added to a stirred solution of 3-bromoacetophenone **13a** (20 g, 100 mmol) and NH₄Cl (11 g, 200 mmol) in 7 N NH₃/MeOH (400 mL). The mixture was stirred at rt for 4 days. Then the solvent was evaporated in vacuo and the residue was taken up in EtOAc (100 mL). The solid was filtered, and the filtrate was evaporated in vacuo to yield intermediate **rac**-**14a** (20 g, 86% yield), which was used in the next step without further purification. ¹H NMR (360 MHz, DMSO-*d*₆) δ 7.78 (t, $J = 1.8$ Hz, 1H), 7.60 (ddd, $J = 0.9, 1.7, 7.9$ Hz, 1H), 7.56 (ddd, $J = 1.1, 1.9, 7.9$ Hz, 1H), 7.39 (t, $J = 8.0$ Hz, 1H), 3.15 (br s, 2H), 1.64 (s, 3H). LC-MS m/z 225 [M + H]⁺.

rac-2-Amino-2-(5-bromo-2-fluorophenyl)propanenitrile (*rac*-14b**).** Starting from 1-(5-bromo-2-fluorophenyl)ethanone (46.3 g, 213 mmol) and following the same procedure as for *rac*-**14a**, the corresponding aminonitrile *rac*-**14b** was obtained (30 g, 60% yield). ¹H NMR (360 MHz, CDCl₃) δ 7.80 (dd, $J = 2.2, 6.9$ Hz, 1H), 7.48 (ddd, $J = 2.5, 4.2, 8.6$ Hz, 1H), 7.03 (dd, $J = 8.6, 10.8$ Hz, 1H), 2.18 (br s, 2H), 1.86 (s, 3H). LC-MS m/z 243 [M + H]⁺.

rac-2-Amino-2-(3-bromophenyl)-propionic Acid (*rac*-15a**).** Intermediate *rac*-**14a** (47 g, 209 mmol) was dissolved in acetic acid (250 mL), and HCl (37% in water, 240 mL) was added. Then the mixture was refluxed for 16 h, after which the reaction mixture was concentrated in vacuo.

Water was added, and the aqueous layer was washed with EtOAc. Then the aqueous layer was adjusted to pH 7 by slow addition of 25% aq NaOH solution. The resulting solid was filtered, washed with water and diethyl ether, and dried under vacuum at 50 °C to yield intermediate *rac*-**15a** (36 g, 71% yield). LC-MS m/z 242 [M - H]⁻. NMR shifts were in accordance to those reported previously.³⁷

rac-2-Amino-2-(5-bromo-2-fluorophenyl)propanoic Acid (*rac*-15b**).** Starting from *rac*-**14b** (19.9 g, 81.9 mmol) and following the same procedure as for *rac*-**15a**, the corresponding aminonitrile *rac*-**15b** was obtained (14.6 g, 68% yield). ¹H NMR (360 MHz, DMSO-*d*₆) δ 7.78 (br s, 1H), 7.64 (dd, $J = 2.6, 6.9$ Hz, 1H), 7.55 (ddd, $J = 2.6, 4.2, 8.6$ Hz, 1H), 7.18 (dd, $J = 8.6, 11.2$ Hz, 1H), 1.64 (s, 3H) (2H exchanged). LC-MS m/z 260 [M + H]⁺.

rac-Methyl 2-Amino-2-(3-bromophenyl)propanoate (*rac*-16a**).** Intermediate *rac*-**15a** (36 g, 147 mmol) was dissolved in MeOH (1 L). Then sulfuric acid (103 mL, 1.93 mol) was added and the reaction mixture was stirred at reflux temperature overnight. After cooling to rt, the solvent was evaporated in vacuo. The residue was dissolved in water, basified with aq NaHCO₃ to pH 8, and extracted with EtOAc. The combined organic layers were dried (MgSO₄), filtered, and evaporated to provide *rac*-**16a** (36 g, 89% yield). ¹H NMR (500 MHz, CDCl₃) δ 7.68 (t, $J = 1.7$ Hz, 1H), 7.37–7.44 (m, 2H), 7.21 (t, $J = 7.8$ Hz, 1H), 3.72 (s, 3H), 1.95 (br s, 2H), 1.68 (s, 3H). LC-MS m/z 258 [M + H]⁺.

rac-Methyl 2-Amino-2-(5-bromo-2-fluorophenyl)propanoate (*rac*-16b**).** Starting from *rac*-**15b** (14.6 g, 55.5 mmol) and following the same procedure as for *rac*-**16a**, the corresponding amino ester *rac*-**16b** was obtained (13.9 g, 87%). ¹H NMR (400 MHz, DMSO-*d*₆) δ ppm 1.27–1.51 (m, 3 H), 2.51 (br s, 2 H), 3.55–3.71 (m, 3 H), 7.12 (dd, $J = 10.9, 8.7$ Hz, 1H), 7.49 (ddd, $J = 8.7, 4.4, 2.5$ Hz, 1H), 7.87 (dd, $J = 7.0, 2.5$ Hz, 1H). LC-MS m/z 276 [M + H]⁺.

(*2R*)-2-Amino-2-(3-bromophenyl)-propan-1-ol (*2R*-17a**).** Ester *rac*-**16a** (7.5 g, 29.1 mmol) was dissolved THF (200 mL) and cooled to -15 °C. Then LAH (1 M in THF; 22 mL, 22 mmol) was added dropwise while stirring. The mixture was left warming up slowly to 0 °C during 1 h. Then more THF (150 mL) was added and satd aq Na₂SO₄ was added dropwise until hydrogen evolution ceased. Then anhydrous Na₂SO₄ was added and the stirring was continued overnight at rt. The mixture was filtered over Celite, rinsed with THF, and the solvent evaporated in vacuo. The crude product was purified by flash column chromatography (silica; 7 N solution of ammonia in MeOH/DCM 0/100 to 3/97). The desired fractions were collected and concentrated in vacuo to yield *rac*-**17a** (5.70 g, 85% yield) as an oil. ¹H NMR (500 MHz, CDCl₃) δ 7.64 (t, $J = 1.9$ Hz, 1H), 7.38–7.44 (m, 2H), 7.25 (t, $J = 7.8$ Hz, 1H), 3.64 (d, $J = 10.7$ Hz, 1H), 3.59 (d, $J = 10.7$ Hz, 1H), 1.81 (br s, 3H), 1.46 (s, 3H). LC-MS m/z 230 [M + H]⁺.

Intermediate *rac*-**17a** (18.0 g) was separated into the corresponding enantiomers by preparative SFC on a Chiraldak Diacel AD 20 mm × 250 mm column using CO₂ and MeOH with 0.2% iPrNH₂ as mobile phase to yield amino alcohol *2R*-**17a** (7.21 g, 40% yield). ¹H NMR (400 MHz, CDCl₃) δ 7.63 (t, $J = 1.8$ Hz, 1H), 7.38–7.43 (m, 2H), 7.25 (t, $J = 7.9$ Hz, 1H), 3.64 (d, $J = 10.7$ Hz, 1H), 3.58 (d, $J = 10.7$ Hz, 1H), 1.78 (br s, 3H), 1.45 (s, 3H). LC-MS m/z 230 [M + H]⁺; $[\alpha]^{20}_{\text{D}} = -14.9$ ($c = 0.29$ in MeOH).

(*2R*)-2-Amino-2-(5-bromo-2-fluorophenyl)propan-1-ol (*2R*-17b**).** Starting from *rac*-**16b** (14.2 g, 48.4 mmol) and following the same procedure as for *rac*-**17a**, the corresponding aminonitrile *rac*-**17b** was obtained (12.0 g, 96% yield). ¹H NMR (400 MHz, CDCl₃) δ 7.63 (dd, $J = 2.5, 7.4$ Hz, 1H), 7.36 (ddd, $J = 2.5, 4.2, 8.5$ Hz, 1H), 6.93 (dd, $J = 8.5, 11.8$ Hz, 1H), 3.82 (d, $J = 10.6$ Hz, 1H), 3.64 (dd, $J = 1.2, 10.6$ Hz, 1H), 1.89 (br s, 3H), 1.48 (d, $J = 0.9$ Hz, 3H). LC-MS m/z 248 [M + H]⁺.

rac-**17b** (16.6 g, 66.9 mmol) was purified by chiral SFC on (Chiraldak AD-H 5 μm 250 mm × 20 mm). Mobile phase (0.3% isopropylamine, 80% CO₂, 20% MeOH), yielding 5.3 g *2R*-**17b** (32% yield). ¹H NMR (500 MHz, CDCl₃) δ 7.62 (dd, $J = 2.6, 7.2$ Hz, 1H), 7.36 (ddd, $J = 2.5, 4.3, 8.6$ Hz, 1H), 6.93 (dd, $J = 8.6, 11.8$ Hz, 1H), 3.83 (d, $J = 10.7$ Hz, 1H), 3.65 (br d, $J = 10.7$ Hz, 1H), 2.61 (br s, 3H), 1.48 (s, 3H). LC-MS m/z 248 [M + H]⁺; $[\alpha]^{20}_{\text{D}} = +2.0$ ($c = 0.61$ in DMF).

(*5R*)-5-(3-Bromophenyl)-5-methylmorpholin-3-one (*5R*-18a**).** Chloroacetyl chloride (0.55 mL, 6.95 mmol) was added dropwise to a stirred solution of intermediate *2R*-**17a** (1.6 g, 6.95 mmol) in THF (60 mL) and diisopropylethyl amine (1.44 mL, 8.34 mmol) at -78 °C. The mixture was stirred for 30 min at -78 °C. Then potassium *tert*-butoxide (1.95 g, 17.38 mmol) was added and the mixture was stirred at -15 °C and left warming up to 0 °C during 90 min. The mixture was diluted with satd aq NH₄Cl and extracted with DCM. The organic layer was separated, dried (Na₂SO₄), filtered, and the solvents evaporated in vacuo. The crude product was triturated with Et₂O, filtered, and dried to yield intermediate *5R*-**18a** (1.65 g, 88% yield) as a white solid. ¹H NMR (500 MHz, CDCl₃) δ 7.54 (t, $J = 1.9$ Hz, 1H), 7.46 (td, $J = 1.3, 7.7$ Hz, 1H), 7.31–7.35 (m, 1H), 7.28 (t, $J = 7.5$ Hz, 1H), 6.41 (br s, 1H), 4.19–4.28 (m, 2H), 3.82 (d, $J = 11.8$ Hz, 1H), 3.72 (d, $J = 11.8$ Hz, 1H), 1.67 (s, 3H). LC-MS m/z 311 [M + H]⁺; $[\alpha]^{20}_{\text{D}} = -71.6$ ($c = 0.62$ in DMF); mp = 135.2 °C.

(*5R*)-5-(5-Bromo-2-fluorophenyl)-5-methylmorpholin-3-one (*5R*-18b**).** Starting from *2R*-**17b** (5.1 g, 20.6 mmol) and following the same procedure as for *5R*-**18a**, the corresponding morpholinone *5R*-**18b** was obtained (5.9 g, 89%). ¹H NMR (500 MHz, CDCl₃) δ 7.51 (dd, $J = 2.6, 7.2$ Hz, 1H), 7.43 (ddd, $J = 2.6, 4.3, 8.7$ Hz, 1H), 6.98 (dd, $J = 8.7, 11.6$ Hz, 1H), 6.60 (br s, 1H), 4.30 (d, $J = 11.8$ Hz, 1H), 4.15–4.26 (m, 2H), 3.72 (d, $J = 11.8$ Hz, 1H), 1.64 (s, 3H). LC-MS m/z 288 [M + H]⁺; $[\alpha]^{20}_{\text{D}} = -53.4$ ($c = 0.67$ in DMF); mp = 161.9 °C.

(*5R*)-5-(3-Bromophenyl)-5-methylmorpholine-3-thione (*5R*-19a**).** THF (40 mL) was added to a mixture of intermediate *5R*-**18a** (1.14 g, 3.92 mmol) and phosphorus pentasulfide (0.704 g, 3.17 mmol) at rt. The mixture was stirred at 50 °C for 50 min. Then the mixture was cooled to rt and filtered over cotton and evaporated in vacuo. The crude product was purified by flash column chromatography (silica; DCM). The desired fractions were collected and evaporated in vacuo to yield the thioamide *5R*-**19a** (1.05 g, 93% yield) as a yellow solid. ¹H NMR (500 MHz, CDCl₃) δ 8.44 (br s, 1H), 7.45–7.52 (m, 2H), 7.26–7.33 (m, 2H), 4.56–4.65 (m, 2H), 3.86 (d, $J = 11.8$ Hz, 1H), 3.77 (d, $J = 11.8$ Hz, 1H), 1.71 (s, 3H). LC-MS m/z 286 [M + H]⁺; $[\alpha]^{20}_{\text{D}} = -190.0$ ($c = 0.6$ in DMF).

(*5R*)-5-(5-Bromo-2-fluorophenyl)-5-methylmorpholine-3-thione (*5R*-19b**).** Starting from *5R*-**18b** (5.3 g, 18.4 mmol) and following the same procedure as for *5R*-**19a**, the corresponding thione *5R*-**19b** was obtained (4.1 g, 72% yield). ¹H NMR (400 MHz, CDCl₃) δ 8.48 (br s, 1H), 7.46 (ddd, $J = 2.5, 4.4, 8.5$ Hz, 1H), 7.41 (dd, $J = 2.4, 7.0$ Hz, 1H), 7.01 (dd, $J = 8.5, 11.6$ Hz, 1H), 4.62 (d, $J = 18.4$ Hz, 1H), 4.54 (d, $J = 18.4$ Hz, 1H), 4.33 (d, $J = 12.0$ Hz, 1H), 3.74 (d, $J = 12.0$ Hz, 1H), 1.69 (d, $J = 0.9$ Hz, 3H). LC-MS m/z 304 [M + H]⁺; $[\alpha]^{20}_{\text{D}} = -167.3$ ($c = 0.6$ in DMF).

(*5R*)-5-(3-Bromophenyl)-5-methyl-5,6-dihydro-2H-1,4-oxazin-3-amine Trifluoroacetate Salt (*5R*-20a**).** The thioamide *5R*-**19a** (0.205 g, 0.716 mmol) and 32% aqueous ammonia solution (12 mL) were stirred

in a sealed tube at 60 °C for 4 h. After cooling, the mixture was diluted with water and extracted with DCM. The organic layer was separated, dried (Na_2SO_4), filtered, and the solvent evaporated in vacuo. DCM (15 mL) and TFA (0.25 mL) were added, and the mixture was concentrated in vacuo. To this residue, Et_2O and heptane were added and evaporated. Diisopropyl ether was added, and the suspension was sonicated for 20 min and then stirred overnight at rt. The white precipitate was filtered and washed with diisopropyl ether and dried in vacuo to yield intermediate **5R-20a** (0.19 g, 69% yield) as a white solid. ^1H NMR (400 MHz, CDCl_3) δ 7.57 (t, J = 1.7 Hz, 1H), 7.36 (td, J = 0.9, 7.9 Hz, 1H), 7.32 (br d, J = 7.90 Hz, 1H), 7.20 (t, J = 7.90 Hz, 1H), 4.13 (d, J = 15.5 Hz, 1H), 4.05 (d, J = 15.5 Hz, 1H), 3.68 (d, J = 11.3 Hz, 1H), 3.56 (d, J = 11.3 Hz, 1H), 3.32 (br s, 2H), 1.50 (s, 3H). LC-MS m/z 269 [M + H]⁺; $[\alpha]^{20}_{\text{D}} = -112.6$ (c = 0.66 in DMF).

(5R)-5-(5-Bromo-2-fluorophenyl)-5-methyl-5,6-dihydro-2H-1,4-oxazin-3-amine (5R-20b). Starting from **5R-19b** (4.1 g, 13.5 mmol) and following the same procedure as for **5R-20a** the corresponding oxazinamine **5R-20b** was obtained (4.1 g, 87% yield). ^1H NMR (500 MHz, CDCl_3) δ 7.70 (dd, J = 2.6, 6.9 Hz, 1H), 7.32 (ddd, J = 2.6, 4.1, 8.6 Hz, 1H), 6.90 (dd, J = 8.5, 11.4 Hz, 1H), 4.21 (br s, 2H), 4.11 (d, J = 15.6 Hz, 1H), 4.03 (d, J = 15.6 Hz, 1H), 3.86 (dd, J = 1.4, 11.3 Hz, 1H), 3.77 (d, J = 11.5 Hz, 1H), 1.54 (d, J = 0.9 Hz, 3H). LC-MS m/z 287 [M + H]⁺.

(5R)-5-(3-Aminophenyl)-5-methyl-5,6-dihydro-2H-1,4-oxazin-3-amine (5R-21a). Toluene (1.5 mL) was added to a mixture of intermediate **5R-20a** (0.05 g, 0.13 mmol), tris(dibenzylideneacetone)-dipalladium(0) (0.012 g, 0.013 mmol), *rac*-2,2'-bis(diphenylphosphino)-1,1'-binaphthyl (0.024 g, 0.04 mmol), and sodium *tert*-butoxide (0.031 g, 0.326 mmol) in a sealed tube and under nitrogen at rt. The mixture was flushed with nitrogen for a few min and then benzophenone imine (0.028 mL, 0.17 mmol) was added and the mixture was stirred at 80 °C for 7 h. After cooling, a mixture of 1 N HCl/THF (1/1.4 mL) was added and the mixture was stirred at rt overnight. The mixture was diluted with water and washed with EtOAc. The aqueous layer was basified with satd aq Na_2CO_3 and extracted with DCM/EtOH 9/1 (10 times). The combined organic layers were dried (Na_2SO_4), filtered, and the solvents evaporated in vacuo. The crude product was purified by flash column chromatography (silica; 7 N solution of ammonia in MeOH/DCM 0/100 to 8/92). The desired fractions were collected and concentrated in vacuo to yield intermediate **5R-21a** (0.012 g, 45% yield) as an oil. ^1H NMR (500 MHz, CDCl_3) δ 7.12 (t, J = 7.9 Hz, 1H), 6.75–6.80 (m, 2H), 6.56 (br d, J = 7.6 Hz, 1H), 4.13 (d, J = 15.4 Hz, 1H), 4.06 (d, J = 15.4 Hz, 1H), 3.68 (d, J = 11.6 Hz, 1H), 3.60–3.75 (m, 2H), 3.57 (d, J = 11.6 Hz, 1H), 3.09 (br s, 2H), 1.50 (s, 3H). LC-MS m/z 206 [M + H]⁺.

(5R)-5-(5-Amino-2-fluorophenyl)-5-methyl-5,6-dihydro-2H-1,4-oxazin-3-amine (5R-21b). Toluene (1.5 mL) was added to a mixture of intermediate **5R-20b** (3.2 g, 11.1 mmol), tris(dibenzylideneacetone)-dipalladium(0) (1.02 g, 1.11 mmol), *rac*-2,2'-bis(diphenylphosphino)-1,1'-binaphthyl (2.08 g, 3.34 mmol), and sodium *tert*-butoxide (1.93 g, 20.1 mmol) in a sealed tube and under nitrogen at rt. The mixture was flushed with nitrogen for a few minutes and then benzophenone imine (3.74 mL, 22.3 mmol) was added and the mixture was stirred at 100 °C for 2 h. After cooling, the mixture was diluted with water and extracted with DCM. The organic layer was dried (Na_2SO_4), filtered, and the solvents concentrated in vacuo. The crude product was purified by flash column chromatography (silica; 7 N solution of ammonia in MeOH/DCM 0/100 to 3/97). The desired fractions were collected and concentrated in vacuo to yield the intermediate benzophenone imine as a yellow foam (3.6 g, 83% yield). This imine (3.6 g, 9.29 mmol) was dissolved in HCl (0.6 M in 2-propanol, 66 mL), and the resulting mixture was stirred at rt for 30 min. Diethyl ether (400 mL) was added, and the precipitated product (HCl salt of **5R-21b**) was filtered and washed with ether. ^1H NMR (400 MHz, $\text{DMSO}-d_6$) δ ppm 1.61 (s, 3 H), 3.81–3.89 (m, 1H), 4.08 (d, J = 12.0 Hz, 1H), 4.48–4.61 (m, 2H), 6.63–6.88 (m, 3 H), 7.03 (br dd, J = 12.1, 8.4 Hz, 2H), 8.62 (s, 1 H), 9.26 (s, 1 H), 10.76 (s, 1 H). Because the HCl salt of **5R-21b** was hygroscopic, the base was liberated prior to the next step. Hence **5R-21b** was dissolved in MeOH and excess 7 N solution of ammonia in MeOH was added. Then all volatiles were evaporated in vacuo. The residue was purified by flash column chromatography (silica; 7 N solution of

ammonia in MeOH 1/99 to 12/88). The desired fractions were collected and concentrated in vacuo to yield **5R-21b** as an off white solid (1.6 g, 77%). LC-MS m/z 224 [M + H]⁺.

(3R)-3-(5-Bromo-2-fluorophenyl)-3-methylmorpholine-2,5-dione (3R-22). Enantiopure **5R-15a** was obtained via preparative SFC of *rac*-**15a** on a Chiralpak Diacel AD 20 mm × 250 mm column using CO_2 and MeOH with 0.2% iPrNH₂ as mobile phase. To a cooled solution of intermediate **5R-15b** (41.3 g, 145 mmol) in water (150 mL), a solution of chloroacetyl chloride (24 mL, 304.5 mmol) in 1,4-dioxane (75 mL) was added dropwise. Simultaneously, NaOH (5 M in water, 29 mL) was added to adjust the pH at 10–11. The reaction mixture was stirred at rt for 2 h. The organic layer was separated, and the aqueous layer extracted with Et_2O . Then the aqueous layer was acidified with HCl (6 M in water) until pH 2. The precipitated white solid was collected by filtration, washed with water, and dried. The obtained intermediate (42 g, 124 mmol) and NaHCO_3 (20.8 g, 248 mmol) were dissolved in DMF (1000 mL), and the reaction mixture was stirred at 80 °C for 3 h. The mixture was partially concentrated in vacuo, cooled to rt, and then filtered over Celite. The filtrate was concentrated in vacuo, and the residue was purified by flash column chromatography (silica; MeOH/DCM 0/100 to 5/95). The desired fractions were collected and concentrated in vacuo to yield intermediate **3R-22** (36 g, 96% yield). ^1H NMR (400 MHz, $\text{DMSO}-d_6$) δ 9.12 (br s, 1H), 7.68 (ddd, J = 2.5, 4.4, 8.7 Hz, 1H), 7.63 (dd, J = 2.5, 6.9 Hz, 1H), 7.29 (dd, J = 8.7, 11.2 Hz, 1H), 4.97 (d, J = 16.4 Hz, 1H), 4.74 (d, J = 16.4 Hz, 1H), 1.84 (s, 3H). LC-MS m/z 302 [M + H]⁺; $[\alpha]^{20}_{\text{D}} = +31.6$ (c = 0.53 in DMF); mp = 162.6 °C.

(5R)-5-(5-Bromo-2-fluorophenyl)-6-fluoro-5-methylmorpholin-3-one (5R-23). A solution of intermediate **3R-22** (10 g, 21.5 mmol) in THF (105 mL) was cooled to –78 °C under N_2 atmosphere. Then diisobutylaluminum hydride (1 M in toluene, 43 mL, 43 mmol) was slowly added. The reaction mixture was allowed to reach rt over 2 h. The reaction mixture was cooled down to 0 °C and quenched by the slow addition of aq 1 N HCl solution. The mixture was then extracted with EtOAc, and the organic layers were separated, dried (Na_2SO_4), filtered, and the solvent evaporated in vacuo to yield the hydroxymorpholinone (6.6 g, 100% yield) as a 80:20 mixture of diastereoisomers, which was used as such in the following reaction. The crude hydroxymorpholinone (6.3 g, 20.7 mmol) was dissolved in DCM (84 mL), and the reaction was cooled down to 0 °C. Then DAST (3 mL, 24.9 mmol) was added dropwise. After 20 min at 0 °C, the reaction mixture was quenched with satd aq NaHCO_3 and extracted with DCM. The combined organic layers were dried (MgSO_4), filtered, and the solvent evaporated in vacuo. The crude product was suspended in diisopropyl ether, filtered, and dried in vacuo at 60 °C to yield intermediate **5R-23** (4.2 g, 66% yield) as an 80:20 mixture of *6R* and *6S* isomers. ^1H NMR (400 MHz, $\text{DMSO}-d_6$) δ 8.97 (s, 1H), 7.55–7.68 (m, 1.2H), 7.45 (dd, J = 2.5, 7.3 Hz, 0.8H), 7.29 (dd, J = 8.5, 11.8 Hz, 0.8H), 7.25 (dd, J = 8.5, 12.00 Hz, 0.2H), 6.03 (d, J = 50.9 Hz, 0.8H), 6.01 (d, J = 50.7 Hz, 0.2H), 4.28 (d, J = 16.3 Hz, 0.2H), 4.20 (d, J = 16.4 Hz, 0.2H), 4.19 (d, J = 16.6 Hz, 0.8H), 4.11 (d, J = 16.6 Hz, 0.8H), 1.64 (s, 0.6H), 1.56 (s, 2.4H). LC-MS m/z 306 [M + H]⁺.

(5R)-5-(5-Bromo-2-fluorophenyl)-6-hydroxy-5-methyl-6-(trifluoromethyl)morpholin-3-one (5R-24). To a solution of intermediate **3R-22** (11.6 g, 38.5 mmol) in THF (117 mL) was added tetrabutylammonium difluorotriphenylsilicate (2.08 g, 3.85 mmol). Then (trifluoromethyl)trimethylsilane (12.5 mL, 84.6 mmol) was added dropwise and the reaction mixture was stirred at rt for 20 min. The mixture was quenched with aqueous NaCl and extracted with EtOAc. The combined organic layers were dried (MgSO_4), filtered, and concentrated in vacuo to yield intermediate **5R-24** (14 g, 98% yield) as a 3:1 *6R*/*6S* mixture, which was used as such in the following step. ^1H NMR (500 MHz, $\text{DMSO}-d_6$) δ 8.51 (s, 1H), 8.39 (br s, 1H), 7.57–7.64 (m, 1H), 7.46 (br d, J = 5.5 Hz, 1H), 7.18 (dd, J = 8.8, 12.9 Hz, 1H), 4.31 (d, J = 16.5 Hz, 1H), 4.17 (d, J = 16.5 Hz, 1H), 1.72 (s, 3H). LC-MS m/z 372 [M + H]⁺; mp = 191.2 °C.

(5R)-5-(5-Bromo-2-fluorophenyl)-6-fluoro-5-methyl-6-(trifluoromethyl)morpholin-3-one (5R-25). Intermediate **5R-24** (3.35 g, 9.00 mmol) was suspended in DCM (25 mL), and after cooling the reaction mixture at 0 °C, DAST (1.32 mL, 10.80 mmol) was added

dropwise. The reaction mixture was stirred at 0 °C for 2 h and then quenched with satd aq NaHCO₃. The organic layer was separated, and the aqueous layer was extracted with DCM. The combined organic layers were dried (MgSO₄), filtered, and the solvent evaporated in vacuo. The crude product was purified by flash column chromatography (silica; MeOH/DCM 0/100 to 1/99). The desired fractions were collected and concentrated in vacuo to yield intermediate **5R-25** (3.15 g, 93% yield) as a 25:75 6R/6S mixture as an off-white solid. ¹H NMR (500 MHz, CDCl₃) δ 7.61 (td, *J* = 2.1, 7.1 Hz, 0.25H), 7.48–7.53 (m, 1H), 7.45 (dd, *J* = 2.3, 7.2 Hz, 1H), 7.13 (br s, 1H), 7.00 (dd, *J* = 8.7, 12.1 Hz, 0.25H), 6.99 (dd, *J* = 8.7, 12.4 Hz, 0.75H), 4.52–4.59 (m, 1.25H), 4.48 (d, *J* = 15.9 Hz, 0.75H), 2.00 (s, 0.75H), 1.96 (s, 2.25H). LC-MS *m/z* 374 [M + H]⁺.

(5*R*)-5-(5-Bromo-2-fluorophenyl)-6-chloro-5-methyl-6-(trifluoromethyl)morpholin-3-one (**5R-26**). Intermediate **5R-24** (14 g, 37.6 mmol) was dissolved in DCM (600 mL) and cooled to 0 °C, and then thionyl chloride (11.2 mL, 150 mmol) was added dropwise. The reaction mixture was stirred for 30 min at 0 °C, and then pyridine (18.2 mL, 225.7 mmol) was added. After 30 min, the reaction was hydrolyzed with aq 1 N HCl and then extracted with DCM. The organic layers were separated, dried (MgSO₄), filtered, and evaporated in vacuo. The crude product was purified by flash column chromatography (silica; 7 N solution of ammonia in MeOH/DCM 0/100 to 2/98). The desired fractions were collected and concentrated in vacuo to yield intermediate **5R-26** (6 g, 41% yield) as a mixture of diastereoisomers. ¹H NMR (400 MHz, DMSO-*d*₆) δ 9.10 (br s, 1H), 7.69 (ddd, *J* = 2.5, 3.9, 8.8 Hz, 1H), 7.48–7.62 (m, 1H), 7.27 (dd, *J* = 8.8, 12.9 Hz, 1H), 4.76 (br d, *J* = 16.2 Hz, 1H), 4.42 (dd, *J* = 0.9, 16.8 Hz, 1H), 1.90 (s, 3H). LC-MS *m/z* 390 [M + H]⁺; mp = 147.0 °C.

(5*R*)-5-(5-Bromo-2-fluorophenyl)-5-methyl-6-(trifluoromethyl)morpholin-3-one (**5R-27**). To a solution of intermediate **5R-26** (3 g, 7.68 mmol) in acetic acid (136 mL), zinc (1.26 g, 19.2 mmol) was added. The reaction mixture was then stirred at 80 °C for 3 h, after that, the reaction was filtered hot and concentrated in vacuo. The residue was dissolved in DCM and washed with ammonium hydroxide solution. The organic phase was separated, dried (MgSO₄), and the solvent concentrated in vacuo. The crude product purified by column chromatography (silica; 7 N solution of ammonia in MeOH/DCM 0/100 to 3/97). The desired fractions were collected and concentrated in vacuo to yield intermediate **5R-27** (2.7 g, 99% yield). ¹H NMR (400 MHz, CDCl₃) δ 7.42–7.52 (m, 2H), 7.16 (s, 1H), 6.99 (dd, *J* = 9.1, 11.9 Hz, 1H), 4.48 (d, *J* = 17.1 Hz, 1H), 4.34 (d, *J* = 17.1 Hz, 1H), 1.92 (d, *J* = 0.7 Hz, 3H). LC-MS *m/z* 356 [M + H]⁺.

(5*R*)-5-(5-Bromo-2-fluorophenyl)-6-fluoro-5-methylmorpholine-3-thione (**5R-28**). THF (100 mL) was added to a mixture of intermediate **5R-23** (4.20 g, 13.7 mmol) and phosphorus pentasulfide (3.66 g, 16.5 mmol) at rt. The mixture was stirred at 70 °C for 3 h. Then the mixture was cooled to rt and filtered over cotton and evaporated in vacuo. The crude product was purified by flash column chromatography (silica; EtOAc/heptane 0/1 to 1/0). The desired fractions were collected and evaporated in vacuo to yield the thioamide **5R-28** as a yellow solid (3 g, 68% yield, as a 62:38 6R/6S mixture).

(5*R*)-5-(5-Bromo-2-fluorophenyl)-6-fluoro-5-methyl-6-(trifluoromethyl)morpholine-3-thione (**5R-29**). Starting from **5R-25** (3.05 g, 8.15 mmol) and following the same procedure as for **5R-28**, the corresponding thione **5R-29** was obtained (2.80 g, white foam, 88% yield) as a 25:75 6R/6S mixture. ¹H NMR (500 MHz, DMSO-*d*₆) δ 11.44 (br s, 0.25H), 11.30 (br s, 0.75H), 7.69–7.77 (m, 1H), 7.67 (br d, *J* = 6.9 Hz, 0.25H), 7.60 (dd, *J* = 2.3, 7.2 Hz, 0.75H), 7.30 (dd, *J* = 8.8, 12.6 Hz, 0.75H), 7.27 (dd, *J* = 8.9, 12.7 Hz, 0.25H), 5.07 (d, *J* = 18.2 Hz, 0.25H), 5.05 (d, *J* = 17.9 Hz, 0.75H), 4.78 (d, *J* = 18.2 Hz, 0.25H), 4.74 (d, *J* = 18.2 Hz, 0.75H), 1.92 (br s, 2.25H), 1.90 (br s, 0.75H). LC-MS *m/z* 390 [M + H]⁺.

(5*R*)-5-(5-Bromo-2-fluoro-phenyl)-5-methyl-6-(trifluoromethyl)morpholine-3-thione (**5R-30**). Starting from **5R-27** (9.8 g, 27.5 mmol) and following the same procedure as for **5R-28**, the corresponding thioamide **5R-30** was obtained (9.4 g, white foam, 92% yield) as a 80:20 6R/6S mixture.

(5*R*, 6*S*)-5-(5-Bromo-2-fluorophenyl)-6-fluoro-5-methyl-2,6-dihydro-1,4-oxazin-3-amine ((**5R,6S-31**) and (5*R*,6*R*)-5-(5-Bromo-2-

fluorophenyl)-6-fluoro-5-methyl-2,6-dihydro-1,4-oxazin-3-amine ((**5R,6R-31**). The crude thione **5R-28** (3.0 g, 9.3 mmol) was dissolved in 7 N solution of ammonia in MeOH (150 mL), and the reaction mixture was stirred in a sealed tube at 60 °C for 18 h. Next, the solvent was evaporated and the residue redissolved in 7 N solution of ammonia in MeOH (150 mL) and stirred in a sealed tube at 60 °C for another 18 h. Then the solvent was evaporated and the crude product purified by column chromatography (silica; 7 N solution of ammonia in MeOH/DCM 0/1 to 1/9). The desired fractions were collected and concentrated in vacuo to yield the amidine (**5R,6R-31**) (1.6 g, 56%). ¹H NMR (360 MHz, CDCl₃) δ 8.00 (dd, *J* = 2.6, 6.9 Hz, 1H), 7.35 (ddd, *J* = 2.7, 4.3, 8.7 Hz, 1H), 6.91 (dd, *J* = 8.6, 11.5 Hz, 1H), 6.04 (dd, *J* = 1.8, 51.6 Hz, 1H), 4.34 (br s, 2H), 4.26 (d, *J* = 15.3 Hz, 1H), 4.13 (d, *J* = 15.3 Hz, 1H), 1.51 (t, *J* = 1.5 Hz, 3H). LC-MS *m/z* 305 [M + H]⁺ and (**5R,6S-31**) (0.27 g, 9%). ¹H NMR (360 MHz, CDCl₃) δ 7.44 (dd, *J* = 2.6, 6.9 Hz, 1H), 7.37 (ddd, *J* = 2.7, 4.3, 8.7 Hz, 1H), 6.93 (dd, *J* = 8.6, 11.5 Hz, 1H), 5.98 (d, *J* = 51.9 Hz, 1H), 4.43 (br s, 2H), 4.25 (d, *J* = 15.7 Hz, 1H), 3.99 (d, *J* = 15.7 Hz, 1H), 1.61 (t, *J* = 2.0 Hz, 3H). LC-MS *m/z* 305 [M + H]⁺.

(5*R*,6*S*)-5-(5-Bromo-2-fluorophenyl)-6-fluoro-5-methyl-6-(trifluoromethyl)-5,6-dihydro-2H-1,4-oxazin-3-amine ((**5R,6S-32**) and (5*R*,6*R*)-5-(5-Bromo-2-fluorophenyl)-6-fluoro-5-methyl-6-(trifluoromethyl)-5,6-dihydro-2H-1,4-oxazin-3-amine ((**5R,6R-32**). Starting from **5R-27** (10 g, 25.6 mmol) and following the same procedure as for **5R-28**, both diastereomers of **32** were separately isolated (**5R,6S-32** (2.0 g, 21% yield). ¹H NMR (400 MHz, CDCl₃) δ 7.44 (dd, *J* = 2.5, 7.3 Hz, 1H), 7.40 (ddd, *J* = 2.5, 4.0, 8.5 Hz, 1H), 6.89 (dd, *J* = 8.7, 12.4 Hz, 1H), 4.25–4.55 (m, 4H), 1.79 (s, 3H). LC-MS *m/z* 305 [M + H]⁺ and (**5R,6R-32**) (0.75 g, 8% yield). ¹H NMR (400 MHz, CDCl₃) δ 7.58 (td, *J* = 2.4, 7.0 Hz, 1H), 7.38 (ddd, *J* = 2.6, 4.0, 8.7 Hz, 1H), 6.89 (dd, *J* = 8.8, 12.0 Hz, 1H), 4.50 (d, *J* = 15.4 Hz, 1H), 4.43 (d, *J* = 15.3 Hz, 1H), 4.35 (br s, 2H), 1.74–1.81 (m, 3H). LC-MS *m/z* 373 [M + H]⁺.

(5*R*,6*R*)-5-(5-Bromo-2-fluorophenyl)-5-methyl-6-(trifluoromethyl)-2,6-dihydro-1,4-oxazin-3-amine ((**5R,6R-33**) and (5*R*,6*S*)-5-(5-Bromo-2-fluorophenyl)-5-methyl-6-(trifluoromethyl)-2,6-dihydro-1,4-oxazin-3-amine ((**5R,6S-33**). Starting from **5R-30** (6 g, 16.1 mmol) and following the same procedure as for (**5R,6R-31**), the corresponding amidine diastereomers of **33** were separately isolated (**5R,6R-33** (3.4 g, 59% yield). ¹H NMR (400 MHz, CDCl₃) δ 8.02 (dd, *J* = 2.6, 7.1 Hz, 1H), 7.36 (ddd, *J* = 2.4, 4.2, 8.7 Hz, 1H), 6.89 (dd, *J* = 8.7, 11.5 Hz, 1H), 4.59 (dq, *J* = 1.1, 8.3 Hz, 1H), 4.32 (br s, 2H), 4.20 (d, *J* = 0.8 Hz, 2H), 1.64 (d, *J* = 1.2 Hz, 3H). LC-MS *m/z* 355 [M + H]⁺; [a]²⁰_D = -66.5 (*c* = 1.23 in DMF). (**5R,6S-33**) (0.75 g, 13% yield), which was isolated in impure form.

(5*R*,6*R*)-5-(5-Amino-2-fluorophenyl)-6-fluoro-5-methyl-5,6-dihydro-2H-1,4-oxazin-3-amine ((**5R,6R-34**). Bromide (**5R,6R-31**) (1.6 g, 5.24 mmol) was combined with NaN₃ (0.85 g, 13 mmol), CuI (1.25 g, 6.5 mmol), and Na₂CO₃ (1.1 g, 10.5 mmol) in DMSO (75 mL), and the reaction was degassed. After that, *N,N'*-dimethylethylenediamine (1 mL, 9.1 mmol) was added and the mixture was heated at 110 °C for 4 h. The reaction mixture was poured into DCM. Ammonium hydroxide (28% in water) was added, and the organic layer was separated and washed three times with ammonium hydroxide. Then the organic layer was dried (MgSO₄), filtered, and concentrated in vacuo. The crude product was purified by column chromatography (silica; 7 N solution of ammonia in MeOH in DCM 0/100 to 10/90). The desired fractions were collected and concentrated in vacuo to yield the corresponding aniline (**5R,6R-34**) (0.3 g, 24% yield). ¹H NMR (400 MHz, CDCl₃) δ 6.83 (dd, *J* = 8.5, 11.8 Hz, 1H), 6.62 (dd, *J* = 2.9, 6.6 Hz, 1H), 6.53 (td, *J* = 3.3, 8.5 Hz, 1H), 6.02 (d, *J* = 52.5 Hz, 1H), 4.42 (br s, 2H), 4.22 (dd, *J* = 0.7, 15.5 Hz, 1H), 3.97 (d, *J* = 15.5 Hz, 1H), 3.56 (br s, 2H), 1.60 (t, *J* = 2.0 Hz, 3H). LC-MS *m/z* 242 [M + H]⁺.

(5*R*,6*S*)-5-(5-Amino-2-fluorophenyl)-6-fluoro-5-methyl-5,6-dihydro-2H-1,4-oxazin-3-amine ((**5R,6S-34**). Starting from (**5R,6S-31**) (0.27 g) and following the same procedure as for (**5R,6R-34**), the corresponding (**5R,6S-34**) was obtained (0.040 g, 15% yield). ¹H NMR (360 MHz, CDCl₃) δ 7.22 (dd, *J* = 3.1, 6.8 Hz, 1H), 6.81 (dd, *J* = 8.4, 11.7 Hz, 1H), 6.45–6.54 (m, 1H), 6.05 (dd, *J* = 1.5, 51.9 Hz, 1H), 4.70 (br s, 2H), 4.25 (d, *J* = 15.5 Hz, 1H), 4.11 (d, *J* = 15.5 Hz, 1H), 3.56 (br s, 2H), 1.48–1.53 (m, 3H).

(5R,6S)-5-(5-Amino-2-fluorophenyl)-6-fluoro-5-methyl-6-(trifluoromethyl)-5,6-dihydro-2H-1,4-oxazin-3-amine ((5R,6S)-35). Starting from (5R,6S)-32 (2.0 g, 5.36 mmol) and following the same procedure as for (5R,6R)-34, the corresponding (5R,6S)-35 was obtained (1.3 g, 78% yield). ¹H NMR (360 MHz, CDCl₃) δ 6.80 (dd, *J* = 8.6, 12.6 Hz, 1H), 6.64 (dd, *J* = 2.2, 6.6 Hz, 1H), 6.59 (td, *J* = 3.0, 8.2 Hz, 1H), 4.36–4.49 (m, 2H), 4.31 (br s, 2H), 3.51 (br s, 2H), 1.73–1.84 (m, 3H); [a]_D²⁰ = +95.8 (*c* = 0.3 in MeOH).

(5R,6R)-5-(5-Amino-2-fluorophenyl)-6-fluoro-5-methyl-6-(trifluoromethyl)-5,6-dihydro-2H-1,4-oxazin-3-amine ((5R,6R)-35). Starting from (5R,6R)-32 (1.1 g, 2.95 mmol) and following the same procedure as for (5R,6R)-34, the corresponding (5R,6R)-35 was obtained (0.75 g, 82% yield). ¹H NMR (360 MHz, CDCl₃) δ 6.73–6.85 (m, 2H), 6.58 (td, *J* = 3.2, 8.6 Hz, 1H), 4.49 (d, *J* = 15.7 Hz, 1H), 4.42 (d, *J* = 15.7 Hz, 1H), 4.31 (br s, 2H), 3.51 (br s, 2H), 1.77 (s, 3H). LC-MS *m/z* 310 [M + H]⁺.

(5R,6R)-5-(5-Amino-2-fluorophenyl)-5-methyl-6-(trifluoromethyl)-5,6-dihydro-2H-1,4-oxazin-3-amine ((5R,6R)-36). Starting from (5R,6R)-33 (3.4 g, 9.57 mmol) and following the same procedure as for (5R,6R)-34, the corresponding (5R,6R)-36 was obtained (2.5 g, 90% yield). ¹H NMR (360 MHz, CDCl₃) δ 7.20 (dd, *J* = 2.9, 6.6 Hz, 1H), 6.80 (dd, *J* = 8.6, 11.9 Hz, 1H), 6.54 (td, *J* = 3.6, 8.6 Hz, 1H), 4.61 (q, *J* = 8.4 Hz, 1H), 4.27 (br s, 2H), 4.20 (s, 2H), 3.56 (br s, 2H), 1.64 (s, 3H). LC-MS *m/z* 292 [M + H]⁺; [a]_D²⁰ = -94.9 (*c* = 0.42 in MeOH).

(5R,6S)-5-(5-Amino-2-fluorophenyl)-5-methyl-6-(trifluoromethyl)-5,6-dihydro-2H-1,4-oxazin-3-amine ((5R,6S)-36). Starting from (5R,6S)-33 (0.3 g, 0.84 mmol) and following the same procedure as for (5R,6R)-34, the corresponding (5R,6S)-36 was obtained (0.10 g, 41% yield). LC-MS *m/z* 292 [M + H]⁺.

Methyl 2-(5-Bromo-2-fluorophenyl)-2-oxoacetate (37). Thionyl chloride (37 mL, 510 mmol) was added dropwise to a stirred solution of (2)-(5-bromo-2-fluoro-phenyl)-2-oxo-acetic acid (42 g, 170 mmol) in MeOH (456 mL) at 0 °C. The mixture was refluxed for 18 h. The solvents were evaporated in vacuo, and the residue was partitioned between satd aq Na₂CO₃ and DCM. The organic layer was separated, dried (MgSO₄), filtered, and concentrated in vacuo to yield 37 (30 g, 68% yield) as a yellow oil.

Isopropyl 2-(5-Bromo-2-fluoro-phenyl)-2-[(S)-tert-butylsulfinyl]imino-acetate (S-38). Titanium(IV) isopropoxide (51.6 mL, 172 mmol) was added to a stirred mixture of 37 (30 g, 115 mmol) and (S)-2-methyl-2-propanesulfinamide (16.7 g, 138 mmol) in *n*-heptane (1000 mL). The mixture was stirred at 80 °C for 24 h. The mixture was partly concentrated in vacuo then diluted with EtOAc. The mixture was cooled to rt, and water was added. The resulting mixture was filtered through a pad of Celite and rinsed with EtOAc and water. The organic layer was separated, dried (MgSO₄), filtered, and concentrated in vacuo. The residue was purified by flash column chromatography (silica; EtOAc/heptane 0/100 to 50/50). The desired fractions were collected and concentrated in vacuo to yield intermediate S-38 (40 g, 89% yield). ¹H NMR (400 MHz, CDCl₃) δ 7.92 (dd, *J* = 2.1, 6.2 Hz, 1H), 7.59 (ddd, *J* = 2.5, 4.3, 8.7 Hz, 1H), 7.03 (dd, *J* = 8.8, 10.6 Hz, 1H), 5.29 (spt, *J* = 6.2 Hz, 1H), 1.39 (d, *J* = 6.2 Hz, 3H), 1.38 (d, *J* = 6.2 Hz, 3H), 1.36 (s, 9H). LC-MS *m/z* 392 [M + H]⁺.

Isopropyl (2R)-2-(5-Bromo-2-fluorophenyl)-2-[(S)-tert-butylsulfinyl]amino]-2-cyclopropyl-acetate (2R-39). A solution of cyclopropylmagnesium bromide (174 mL, 0.5 M, 87 mmol) was added dropwise over 45 min to a stirred solution of 24.4 g (62 mmol) iminoester S-38 in DCM (388 mL) at -78 °C. The reaction mixture was stirred at -78 °C for 30 min. Then satd aq NH₄Cl was added and the reaction mixture was warmed to rt. The mixture was extracted with DCM and washed with water. The organic layer was separated and dried with MgSO₄, filtered, and concentrated in vacuo to give intermediate 2R-39 (26.4 g 97% yield). ¹H NMR (400 MHz, CDCl₃) δ 8.01 (dd, *J* = 2.5, 6.5 Hz, 1H), 7.48 (ddd, *J* = 2.3, 4.5, 8.7 Hz, 1H), 6.94 (dd, *J* = 8.7, 10.3 Hz, 1H), 5.13 (spt, *J* = 6.3 Hz, 1H), 4.97 (br s, 1H), 1.48 (tt, *J* = 5.3, 8.2 Hz, 1H), 1.22 (d, *J* = 6.2 Hz, 3H), 1.20 (s, 9H), 1.18 (d, *J* = 6.0 Hz, 3H), 0.78–0.88 (m, 1H), 0.60–0.70 (m, 1H), 0.38–0.54 (m, 2H). LC-MS *m/z* 434 [M + H]⁺.

(2R)-2-Amino-2-(5-bromo-2-fluorophenyl)-2-cyclopropyl-acetic Acid Hydrochloride (2R-40). Intermediate 2R-39 (21 g, 48 mmol) was

dissolved in MeOH (96 mL), and then 1 N NaOH (96 mL, 96 mmol) was added. The reaction mixture was refluxed for 4 h, and then it was allowed to reach rt. The mixture was partitioned between water and EtOAc. The aqueous layer was separated, acidified with 1 N HCl, and extracted with DCM. The combined organic extracts were dried over MgSO₄, filtered, and the solvent was evaporated in vacuo to yield the corresponding carboxylic acid as a white solid (15.5 g, 82% yield). This material was dissolved in dioxane (100 mL), and then HCl (4 N in dioxane, 29.6 mL, 118 mmol) was added dropwise. The resulting solution was stirred at rt for 1 h, and the solvent was removed in vacuo. The residue was suspended in DIPE, filtered, and dried in vacuo to give amino acid 2R-40 (HCl salt) as a white solid (10 g, 88% yield). ¹H NMR (360 MHz, DMSO-*d*₆) δ 14.33 (br s, 1H), 8.86 (br s, 3H), 7.98 (dd, *J* = 2.4, 6.8 Hz, 1H), 7.74 (ddd, *J* = 2.6, 4.4, 8.8 Hz, 1H), 7.35 (dd, *J* = 9.0, 10.8 Hz, 1H), 1.70–1.82 (m, 1H), 0.56–0.92 (m, 4H)). LC-MS *m/z* 286 [M – H]⁻; [a]_D²⁰ = -65.4 (*c* = 0.63 in MeOH).

(3R)-3-(5-Bromo-2-fluorophenyl)-3-cyclopropyl-morpholine-2,5-dione (3R-41). Amino acid 2R-40 (40 g, 123 mmol) was dissolved in THF (370 mL), and then 1 N NaOH (256 mL, 256 mmol) was added. The reaction mixture was cooled down to 0 °C, and then a solution of 2-chloroacetyl chloride (24.5 mL, 308 mmol) in THF (50 mL) was added dropwise over 1 h at 15 °C while aq NaOH was simultaneously added (to maintain the pH around 10–11). After the addition was finished, 12 N HCl was added carefully to the mixture until pH 2. The reaction mixture was concentrated in vacuo, and the resulting precipitate was washed with DIPE and dried in vacuo. The resulting solid was dissolved in DMF (1 L), and then NaHCO₃ (19.8 g, 236 mmol) was added. The reaction mixture was stirred at 80 °C for 6 h. The reaction mixture was partially concentrated in a rotary evaporator and filtered through a pad of Celite to remove the salts. The solvent was removed in vacuo to give morpholine dione 3R-41 as a colorless oil (39 g, 99% yield). ¹H NMR (360 MHz, DMSO-*d*₆) δ 8.74 (br s, 1H), 7.92 (dd, *J* = 2.6, 6.9 Hz, 1H), 7.70 (ddd, *J* = 2.6, 4.8, 8.8 Hz, 1H), 7.32 (dd, *J* = 8.8, 11.0 Hz, 1H), 5.12 (d, *J* = 16.8 Hz, 1H), 4.84 (d, *J* = 16.8 Hz, 1H), 1.62–1.72 (m, 1H), 0.84–0.97 (m, 1H), 0.58–0.73 (m, 2H), 0.41–0.52 (m, 1H). LC-MS *m/z* 328 [M + H]⁺; [a]_D²⁰ = +107.5 (*c* = 0.62 in DMF).

(5R)-5-(5-Bromo-2-fluorophenyl)-5-cyclopropyl-6-fluoro-morpholin-3-one (5R-42). Starting from 3R-41 (7.2 g, 21.94 mmol) and following the same procedure as for 5R-23, the corresponding hemiacetal was obtained as 3:2 mixture of diastereoisomers and further converted to 5R-42 in 92% yield (6.0 g, 3:2 mixture of 6S/6R isomers). Hemiacetal: ¹H NMR (600 MHz, DMSO-*d*₆) δ 8.22 (s, 0.4H), 8.10 (s, 0.6H), 7.61 (dd, *J* = 2.6, 7.0 Hz, 0.6H), 7.53–7.58 (m, 1H), 7.50 (ddd, *J* = 2.5, 4.1, 8.7 Hz, 0.4H), 7.12–7.22 (m, 1H), 6.90 (d, *J* = 4.7 Hz, 0.4H), 5.44 (dd, *J* = 1.2, 4.5 Hz, 0.4H), 5.38 (d, *J* = 5.0 Hz, 0.6H), 4.09 (d, *J* = 16.4 Hz, 0.4H), 4.07 (d, *J* = 16.6 Hz, 0.6H), 3.98 (d, *J* = 16.6 Hz, 0.6H), 3.96 (d, *J* = 16.4 Hz, 0.4H), 1.52–1.65 (m, 1H), 0.43–0.59 (m, 1H), 0.14–0.43 (m, 3H) (1H exchanged). LC-MS *m/z* 330 [M + H]⁺. 5R-42: ¹H NMR (400 MHz, CDCl₃) δ 7.94 (br s, 0.4H), 7.51 (dd, *J* = 2.5, 7.0 Hz, 0.4H), 7.39–7.48 (m, 1.6H), 7.20 (br s, 0.6H), 6.94–7.04 (m, 1H), 6.30 (dd, *J* = 1.5, 51.0 Hz, 0.6H), 6.15 (d, *J* = 49.9 Hz, 0.4H), 4.42 (d, *J* = 16.7 Hz, 0.4H), 4.33 (d, *J* = 17.2 Hz, 0.6H), 4.28 (d, *J* = 16.7 Hz, 0.4H), 4.14 (d, *J* = 17.2 Hz, 0.6H), 1.58–1.68 (m, 1H), 0.22–0.74 (m, 4H)). LC-MS *m/z* 332 [M + H]⁺. This material was used as a diasteromeric mixture in the following step.

(5R)-5-(5-Bromo-2-fluorophenyl)-5-cyclopropyl-6-fluoromorpholine-3-thione (5R-43). Starting from 5R-42 (3.0 g, 9 mmol) and following the same procedure as for 5R-28, the corresponding thioamide 5R-43 was obtained (2.8 g, 89% yield) as a mixture of diastereoisomers, which was used as such for the next reaction step.

(5R,6R)-5-(5-Bromo-2-fluorophenyl)-5-cyclopropyl-6-fluoro-2,6-dihydro-1,4-oxazin-3-amine ((5R,6R)-44). Starting from 5R-43 (2.8 g) and following the same procedure as for (5R,6R)-31, the corresponding both diastereomers (5R,6R)-44 (0.98 g, 37% yield) and (5R,6S)-44 (1.16 g, 44% yield) were obtained. (5R,6R)-44: ¹H NMR (360 MHz, CDCl₃) δ 7.29–7.39 (m, 2H), 6.94 (dd, *J* = 8.8, 11.7 Hz, 1H), 6.14 (d, *J* = 52.0 Hz, 1H), 4.37 (br s, 2H), 4.20 (d, *J* = 15.4 Hz, 1H), 3.95 (d, *J* = 15.4 Hz, 1H), 1.59 (dq, *J* = 4.9, 8.6 Hz, 1H), 0.39–0.59 (m, 2H), 0.29–0.38 (m, 1H), 0.14–0.24 (m, 1H). LC-MS *m/z* 331 [M + H]⁺. (5R,6S)-44: ¹H NMR (360 MHz, CDCl₃) δ 7.94 (dd, *J* = 2.6, 6.95 Hz, 1H), 7.35

(ddd, $J = 2.9, 4.2, 8.6$ Hz, 1H), 6.93 (dd, $J = 8.6, 11.5$ Hz, 1H), 6.18 (dd, $J = 2.2, 51.2$ Hz, 1H), 4.29 (br s, 2H), 4.23 (d, $J = 15.4$ Hz, 1H), 4.09 (d, $J = 15.4$ Hz, 1H), 1.45 (dtt, $J = 2.6, 5.4, 8.1$ Hz, 1H), 0.37–0.50 (m, 1H), 0.13–0.33 (m, 3H). LC-MS m/z 331 [M + H]⁺.

(5R,6R)-5-(5-Amino-2-fluorophenyl)-5-cyclopropyl-6-fluoro-2,6-dihydro-1,4-oxazin-3-amine (5R,6R)-45. Starting from (5R,6R)-44 (1.7 g, 5.1 mmol) and following the same procedure as for (5R,6R)-34, the corresponding (5R,6R)-45 was obtained (0.81 g, 59% yield). ¹H NMR (400 MHz, CDCl₃) δ 6.83 (dd, $J = 9.0, 11.8$ Hz, 1H), 6.48–6.56 (m, 2H), 6.18 (d, $J = 52.7$ Hz, 1H), 4.17 (dd, $J = 1.1, 15.4$ Hz, 1H), 3.92 (d, $J = 15.3$ Hz, 1H), 3.53 (br s, 2H), 1.60 (dq, $J = 5.0, 8.4$ Hz, 1H), 0.39–0.54 (m, 2H), 0.31–0.39 (m, 1H), 0.16–0.25 (m, 1H) (2H exchanged). LC-MS m/z 268 [M + H]⁺.

rac-2-Amino-2-(4-bromopyridin-2-yl)propanenitrile (rac-47a). Starting from 1-(4-bromo-2-pyridinyl)-ethanone 46a (18 g, 90 mmol) and following the same procedure as for 14a, the corresponding aminonitrile rac-47a was obtained as a white solid (11 g, 54% yield).

rac-2-Amino-2-(2-chloropyridin-4-yl)propanenitrile (rac-47b). Starting from 4-acetyl-2-chloropyridine 46b (18 g, 90 mmol) and following the same procedure as for 14a, the corresponding aminonitrile rac-47b was obtained (11.4 g, 98% yield) as a yellow solid. LC-MS m/z 182 [M + H]⁺.

rac-2-(4-Bromopyridin-2-yl)alaninamide (rac-48a). Nitrile rac-47a (23 g, 101.7 mmol) was dissolved in a solution of 48% HBr in acetic acid (200 mL), and the mixture was refluxed for 12 h. After cooling to rt, EtOAc (40 mL) was added and the precipitate was filtered off and washed with EtOAc (100 mL), then dried to give rac-48a as an off-white solid (25 g, 61% yield).

rac-2-Amino-2-(2-chloro-4-pyridyl)propanamide (rac-48b). Intermediate rac-47b (6 g, 33.04 mmol) was dissolved in HCl (1 M in AcOH, 165 mL) and HBr (33% in AcOH, 25 mL), and the mixture was stirred at 75 °C for 3 h. After cooling to rt, EtOAc (250 mL) was added and the precipitate was filtered off, washed with EtOAc (100 mL), and dried in vacuo to give rac-48b (9.7 g, 81% yield). LC-MS m/z 198 [M – H]⁻.

rac-2-(4-Bromopyridin-2-yl)alanine (rac-49a). First, 1 N NaOH (412 mL, 412 mmol) was added to a solution of rac-48a (33.4 g, 82.4 mmol) in THF (1 L) at rt. The resulting mixture was then stirred at 65 °C for 16 h. Then the reaction mixture was half concentrated, then cooled with an ice bath and brought to pH 7 with 1 N HCl while stirring. A white precipitate formed, which was filtered, washed with diethyl ether, and dried in vacuo to provide rac-49a (13.2 g, 65% yield). ¹H NMR (360 MHz, DMSO-*d*₆) δ 8.39 (d, $J = 5.5$ Hz, 1H), 7.91 (d, $J = 1.5$ Hz, 1H), 7.81 (br s, 3H), 7.60 (dd, $J = 1.8, 5.1$ Hz, 1H), 1.64 (s, 3H). LC-MS m/z 245 [M + H]⁺.

rac-2-Amino-2-(2-chloropyridin-4-yl)propanoic acid (rac-49b). Intermediate rac-48b (9.7 g, 26.84 mmol) was dissolved in NaOH (1 M in water, 134 mL), and the mixture was stirred at rt for 60 h. The reaction mixture was concentrated to half volume in vacuo and then cooled on an ice bath. The pH of the solution was adjusted to pH = 7 by addition of HCl (1 N in water), and a white solid precipitated. The precipitate was filtered off, washed with Et₂O, and dried in vacuo to give intermediate rac-49b (5.48 g, quant yield) as a white solid. ¹H NMR (360 MHz, DMSO-*d*₆) δ 8.38 (d, $J = 5.1$ Hz, 1H), 7.92 (br s, 3H), 7.59 (d, $J = 1.5$ Hz, 1H), 7.50 (dd, $J = 1.5, 5.5$ Hz, 1H), 1.63 (s, 3H). LC-MS m/z 199 [M – H]⁻.

rac-[(2-Amino-2-(4-bromopyridin-2-yl)propanoyl]oxyacetic Acid Trifluoroacetate Salt (rac-51a). Amino acid rac-49a (16.0 g, 65.3 mmol) and Cs₂CO₃ (63.8 g, 195.9 mmol) in dry DMF (500 mL) were stirred for 30 min. Then *tert*-butyl chloroacetate (9.33 mL, 65.3 mmol) was added, and the resulting mixture was stirred at rt for 3 h. Then, ice and DCM were added and the organic layer was separated. The aqueous layer was extracted with DCM. The combined organic layers were dried (MgSO₄), filtered, and evaporated to dryness providing rac-50a as an orange oil (note: a high vacuum of 1–3 mbar is needed to remove a low volatile impurity). Ester rac-50a was dissolved in TFA (234 mL) and stirred at rt for 30 min. Then, the solvent was thoroughly evaporated providing a brown oil, which was treated with diethyl ether and stirred for about 10 min to get white solid which was filtered, washed with diethyl ether, and dried in vacuo at 50 °C to give the TFA salt of rac-51a (8.95 g, 29% yield over two steps). ¹H NMR (360 MHz, DMSO-*d*₆) δ

9.12 (br s, 4H), 8.56 (d, $J = 5.1$ Hz, 1H), 8.10 (d, $J = 1.5$ Hz, 1H), 7.84 (dd, $J = 1.6, 5.3$ Hz, 1H), 4.65–4.87 (m, 2H), 1.95 (s, 3H). LC-MS m/z 303 [M + H]⁺.

rac-[(2-Amino-2-(2-chloropyridin-4-yl)propanoyl]oxyacetic Acid Trifluoroacetate Salt (rac-51b). Starting from rac-49b (5.29 g, 26.36 mmol) and following the same procedure as for rac-51a, the corresponding acid rac-51b was obtained as a trifluoroacetate salt (6.12 g, 96%). ¹H NMR (360 MHz, DMSO-*d*₆) δ 9.50 (br s, 4H), 8.58 (d, $J = 5.4$ Hz, 1H), 7.79 (d, $J = 1.5$ Hz, 1H), 7.65 (dd, $J = 1.5, 5.4$ Hz, 1H), 4.73–4.85 (m, 2H), 1.94 (s, 3H). LC-MS m/z 257 [M – H]⁻.

rac-3-(4-Bromopyridin-2-yl)-3-methylmorpholine-2,5-dione (rac-52a). Amino acid (TFA salt) rac-51a (12.3 g, 29.5 mmol) was suspended in DCM (764 mL) and 2-chloro-1-methylpyridinium iodide (8.3 g, 32.5 mmol) was added, followed by DIPEA (25.3 mL, 88.6 mmol). The reaction mixture was subsequently refluxed for 4 h. Then, the reaction mixture was concentrated in vacuo and purified by column chromatography (silica: heptane/EtOAc 100/0 to 20/80). Evaporation of the product fractions provided 4.6 g rac-52a containing about 30% of impurity bearing a chloro instead of bromo on the pyridine 4-position (55% yield). ¹H NMR (360 MHz, DMSO-*d*₆) δ 9.18 (br s, 1H), 8.44 (d, $J = 5.1$ Hz, 1H), 7.79 (d, $J = 1.5$ Hz, 1H), 7.73 (dd, $J = 1.6, 5.3$ Hz, 1H), 4.62 (s, 2H), 1.74 (s, 3H). LC-MS m/z 285 [M + H]⁺.

rac-3-(2-Chloropyridin-4-yl)-3-methylmorpholine-2,5-dione (rac-52b). Starting from rac-51b (5.29 g, 26.36 mmol) and following the same procedure as for rac-52a, the corresponding acid rac-52b was obtained as white crystals (1.10 g, 19%). ¹H NMR (360 MHz, DMSO-*d*₆) δ 9.43 (br s, 1H), 8.51 (d, $J = 5.4$ Hz, 1H), 7.41–7.43 (m, 1H), 7.39 (dd, $J = 1.6, 5.4$ Hz, 1H), 4.69 (s, 2H), 1.71 (s, 3H). LC-MS m/z 241 [M + H]⁺; mp = 213.5 °C.

rac-(5R*,6R*)-5-(4-Bromo-2-pyridyl)-6-fluoro-5-methylmorpholin-3-one (rac-(5R*,6R*)-53a). Starting from rac-52a (4.3 g, 5.2 mmol) and following the same procedure as for 5R-23, the corresponding rac-(5R*,6R*)-53a was obtained as a single diastereomer (3.55 g, 81%). ¹H NMR (400 MHz, CDCl₃) δ 8.42 (dd, $J = 0.5, 5.3$ Hz, 1H), 7.67 (dd, $J = 0.5, 1.8$ Hz, 1H), 7.42 (dd, $J = 1.8, 5.0$ Hz, 1H), 7.32 (br s, 1H), 6.06 (d, $J = 51.7$ Hz, 1H), 4.38 (d, $J = 17.2$ Hz, 1H), 4.19 (d, $J = 17.2$ Hz, 1H), 1.68 (d, $J = 1.8$ Hz, 3H). LC-MS m/z 289 [M + H]⁺; mp = 193.1 °C.

rac-(5R*,6R*)-5-(2-Chloro-4-pyridyl)-6-fluoro-5-methylmorpholin-3-one (rac-(5R*,6R*)-53b). Starting from rac-52b (1.42 g, 5.90 mmol) and following the same procedure as for 5R-23, the corresponding rac-(5R*,6R*)-53b was obtained as a transparent oil (985 mg, 69%, 65:35 mixture of diastereoisomers). ¹H NMR (360 MHz, CDCl₃) δ 8.46 (d, $J = 5.5$ Hz, 0.35H), 8.46 (d, $J = 5.5$ Hz, 0.65H), 7.64 (br s, 0.65H), 7.60 (br s, 0.35H), 7.39–7.44 (m, 0.35H), 7.32–7.36 (m, 0.65H), 7.28–7.32 (m, 0.35H), 7.22 (dd, $J = 1.3, 5.3$ Hz, 0.65H), 5.65 (d, $J = 50.1$ Hz, 0.65H), 5.51 (d, $J = 49.0$ Hz, 0.35H), 4.45 (d, $J = 16.7$ Hz, 0.35H), 4.37 (d, $J = 16.8$ Hz, 0.65H), 4.34 (d, $J = 16.7$ Hz, 0.35H), 4.22 (d, $J = 16.8$ Hz, 0.65H), 1.78 (d, $J = 1.5$ Hz, 1.05H), 1.70 (d, $J = 1.5$ Hz, 1.95H). LC-MS m/z 245 [M + H]⁺.

rac-(5R*,6R*)-5-(4-Bromopyridin-2-yl)-6-fluoro-5-methylmorpholine-3-thione (rac-(5R*,6R*)-54a). Starting from rac-(5R*,6R*)-53a (3.50 g, 12.11 mmol) and following the same procedure as for 5R-28, the corresponding rac-(5R*,6R*)-54a was obtained as white crystals (2.00 g, 54%). ¹H NMR (360 MHz, CDCl₃) δ 8.43 (br d, $J = 5.1$ Hz, 2H), 7.51 (d, $J = 1.8$ Hz, 1H), 7.45 (dd, $J = 1.8, 5.1$ Hz, 1H), 6.04 (dd, $J = 1.5, 51.6$ Hz, 1H), 4.74 (d, $J = 18.7$ Hz, 1H), 4.62 (d, $J = 18.7$ Hz, 1H), 1.73 (d, $J = 1.8$ Hz, 3H). LC-MS m/z 305 [M + H]⁺.

rac-(5R*,6R*)-5-(2-Chloropyridin-4-yl)-6-fluoro-5-methylmorpholine-3-thione (rac-(5R*,6R*)-54b). Starting from rac-(5R*,6R*)-53b (0.769 g, 1.53 mmol) and following the same procedure as for 5R-28, the corresponding rac-(5R*,6R*)-54b was obtained as a transparent oil (445 mg, 54%, 60:40 mixture of diastereoisomers). LC-MS m/z 259 [M – H]⁻.

rac-(5R*,6R*)-5-(4-Bromopyridin-2-yl)-6-fluoro-5-methyl-5,6-dihydro-2H-1,4-oxazin-3-amine (rac-(5R*,6R*)-55a). Starting from rac-(5R*,6R*)-54a (2.00 g, 6.55 mmol) and following the same procedure as for 5R-31, the corresponding rac-(5R*,6R*)-55a was obtained as white crystals (1.61 g, 85%). ¹H NMR (360 MHz, DMSO-*d*₆) δ 8.45 (d, $J = 5.1$ Hz, 1H), 7.53–7.60 (m, 2H), 6.22 (br s, 2H), 5.97 (d, $J = 53.8$ Hz, 1H), 4.03 (q, $J = 16.0$ Hz, 2H), 1.39 (d, $J = 1.8$ Hz, 3H). LC-MS m/z 288 [M + H]⁺; mp = 125.1 °C.

rac-(*5R*^{*},*6R*^{*})-5-(2-Chloropyridin-4-yl)-6-fluoro-5-methylmorpholine-3-amine (*rac*-**55b**). Starting from *rac*-(*5R*^{*},*6R*^{*})-**54b** (0.445 g, 1.53 mmol) and following the same procedure as for **5R-31**, the corresponding amidine *rac*-(*5R*^{*},*6R*^{*})-**55b** was obtained as a white solid (300 mg, 72%). ¹H NMR (400 MHz, DMSO-*d*₆) δ 8.36 (d, *J* = 5.3 Hz, 1H), 7.45 (d, *J* = 1.5 Hz, 1H), 7.42 (dd, *J* = 1.5, 5.3 Hz, 1H), 6.06 (br s, 2H), 5.88 (d, *J* = 52.2 Hz, 1H), 4.06 (d, *J* = 16.0 Hz, 1H), 3.97 (d, *J* = 16.0 Hz, 1H), 1.40 (d, *J* = 1.8 Hz, 3H). LC-MS *m/z* 245 [M + H]⁺; mp = 174.1 °C. Note: the other diastereoisomer was discarded without NMR analysis.

rac-(*5R*^{*},*6R*^{*})-5-(4-Aminopyridin-2-yl)-6-fluoro-5-methyl-5,6-dihydro-2*H*-1,4-oxazin-3-amine (*rac*-(*5R*^{*},*6R*^{*})-**56a**). Starting from *rac*-(*5R*^{*},*6R*^{*})-**55a** (1.10 g, 3.82 mmol) and following the same procedure as for **5R-34**, the corresponding *rac*-(*5R*^{*},*6R*^{*})-**56a** was obtained as white crystals (0.54 g, 64% yield). LC-MS *m/z* 225 [M + H]⁺.

rac-(*5R*^{*},*6R*^{*})-5-(2-Aminopyridin-4-yl)-6-fluoro-5-methyl-5,6-dihydro-2*H*-1,4-oxazin-3-amine (*rac*-(*5R*^{*},*6R*^{*})-**56b**). Starting from *rac*-(*5R*^{*},*6R*^{*})-**55b** (0.300 g, 1.23 mmol) and following the same procedure as for **5R-34**, the corresponding aniline *rac*-(*5R*^{*},*6R*^{*})-**56b** was obtained as a transparent oil (200 mg, 72%). LC-MS *m/z* 225 [M + H]⁺.

■ ASSOCIATED CONTENT

S Supporting Information

The Supporting Information is available free of charge on the ACS Publications website at DOI: [10.1021/acs.jmedchem.5b01101](https://doi.org/10.1021/acs.jmedchem.5b01101).

Crystal structure experimental data; selection set for p*K*_a calculations; correlation of calculated and experimental p*K*_a; QM calculations on conformation of diastereomers of **7a**; chemical stability assessment of (2*R*,3*R*)-**7a** (PDF)

Molecular formula strings (CSV)

■ AUTHOR INFORMATION

Corresponding Authors

*For F.J.R.R.: phone, +3214608216; E-mail, frombout@its.jnj.com.

*For A.A.T.: phone, +34925245750; E-mail, atrabanc@its.jnj.com.

Author Contributions

The manuscript was written through contributions of all authors. All authors have given approval to the final version of the manuscript.

Notes

The authors declare no competing financial interest.

■ ACKNOWLEDGMENTS

We thank the analytical departments in Beerse and Toledo for helping with compound characterization and purification. We thank Michel Carpentier for performing the chemical stability experiments on (2*R*,3*R*)-**7a**. We also thank Geert Pille and Sigrid Stockbroekx for the physicochemical measurements. Finally, we thank Proteros GMBH for BACE1 crystal growth, soaking, and structure determination of **3R-6a**.

■ ABBREVIATIONS USED

AUC_{0-last}: area under the curve until last time point sampled; A β , amyloid beta; BACE1, beta-site amyloid precursor protein cleaving enzyme 1; BINAP, 2,2'-bis(diphenylphosphino)-1,1'-binaphthyl; C_{max}, maximum plasma concentration; CSF, cerebrospinal fluid; DAST, diethylaminosulfur trifluoride; dLM, dog liver microsomes; DMEDA, *N,N'*-dimethylethylene-diamine; DMTMM, 4-(4,6-dimethoxy-1,3,5-triazin-2-yl)-4-methylmorpholinium chloride; f_w, free (unbound) fraction; HATU, (1-[bis(dimethylamino)methylene]-1*H*-1,2,3-triazolo-

[4,5-*b*]pyridinium 3-oxide hexafluorophosphate); hLM, human liver microsomes; HP β CD, (2-hydroxypropyl)- β -cyclodextrin [128446-35-5]; K_p, brain-to-plasma ratio; nd, not determined; mLML, mouse liver microsomes; P_{app}, apparent permeability; po, per os (= oral); rLM, rat liver microsomes; SBE β CD, sulfobutylether β -cyclodextrin sodium salt [182410-00-0]; sc, subcutaneous; T_{1/2}, half-life; TBAT, tetrabutylammonium difluorotriphenylsilicate; T_{max}, time at which maximum plasma concentration is reached; WT, wild type

■ REFERENCES

- (1) Hebert, L. E.; Weuve, J.; Scherr, P. A.; Evans, D. A. Alzheimer disease in the United States (2010–2050) estimated using the 2010 census. *Neurology* **2013**, *80*, 1778–1783.
- (2) *Dementia*; Fact Sheet 362; World Health Organization: Geneva, 2015; <http://www.who.int/mediacentre/factsheets/fs362/en/> (accessed August 10, 2015).
- (3) Braak, H.; Braak, E. Neuropathological staging of Alzheimer-related changes. *Acta Neuropathol.* **1991**, *82*, 239–259.
- (4) Karan, E.; Mercken, M.; De Strooper, B. The amyloid cascade hypothesis for Alzheimer's disease: an appraisal for the development of therapeutics. *Nat. Rev. Drug Discovery* **2011**, *10*, 698–712.
- (5) Thinakaran, G.; Koo, E. H. Amyloid precursor protein trafficking, processing, and function. *J. Biol. Chem.* **2008**, *283*, 29615–29619.
- (6) Mawuenyega, K. G.; Sigurdson, W.; Ovod, V.; Munsell, L.; Kasten, T.; Morris, J. C.; Yarasheski, K. E.; Bateman, R. J. Decreased clearance of CNS beta-amyloid in Alzheimer's disease. *Science* **2010**, *330*, 1774.
- (7) Greenwald, J.; Riek, R. Biology of amyloid: structure, function, and regulation. *Structure* **2010**, *18*, 1244–1260.
- (8) De Strooper, B.; Vassar, R.; Golde, T. The secretases: enzymes with therapeutic potential in Alzheimer disease. *Nat. Rev. Neurol.* **2010**, *6*, 99–107.
- (9) Vassar, R.; Bennett, B. D.; Babu-Khan, S.; Kahn, S.; Mendiaz, E. A.; Denis, P.; Teplow, D. B.; Ross, S.; Amarante, P.; Loeloff, R.; Luo, Y.; Fisher, S.; Fuller, J.; Edenson, S.; Lile, J.; Jarosinski, M. A.; Biere, A. L.; Curran, E.; Burgess, T.; Louis, J. C.; Collins, F.; Treanor, J.; Rogers, G.; Citron, M. Beta-secretase cleavage of Alzheimer's amyloid precursor protein by the transmembrane aspartic protease BACE. *Science* **1999**, *286*, 735–741.
- (10) Ghosh, A. K.; Osswald, H. L. BACE1 (beta-secretase) inhibitors for the treatment of Alzheimer's disease. *Chem. Soc. Rev.* **2014**, *43*, 6765–6813.
- (11) Butini, S.; Brogi, S.; Novellino, E.; Campiani, G.; Ghosh, A. K.; Brindisi, M.; Gemma, S. The structural evolution of beta-secretase inhibitors: a focus on the development of small-molecule inhibitors. *Curr. Top. Med. Chem.* **2013**, *13*, 1787–1807.
- (12) Edwards, P. D.; Albert, J. S.; Sylvester, M.; Aharony, D.; Andisik, D.; Callaghan, O.; Campbell, J. B.; Carr, R. A.; Chessari, G.; Congreve, M.; Frederickson, M.; Folmer, R. H.; Geschwindner, S.; Koether, G.; Kolmodin, K.; Krumrine, J.; Mauger, R. C.; Murray, C. W.; Olsson, L. L.; Patel, S.; Spear, N.; Tian, G. Application of fragment-based lead generation to the discovery of novel, cyclic amidine beta-secretase inhibitors with nanomolar potency, cellular activity, and high ligand efficiency. *J. Med. Chem.* **2007**, *50*, 5912–5925.
- (13) Baxter, E. W.; Conway, K. A.; Kennis, L.; Bischoff, F.; Mercken, M. H.; De Winter, H. L.; Reynolds, C. H.; Toung, B. A.; Luo, C.; Scott, M. K.; Huang, Y.; Braeken, M.; Pieters, S. M. A.; Berthelot, D. J. C.; Masure, S.; Bruunzeel, W. D.; Jordan, A. D.; Parker, M. H.; Boyd, R. E.; Qu, J.; Alexander, R. S.; Brenneman, D. E.; Reitz, A. B. 2-amino-3,4-dihydroquinazolines as inhibitors of BACE-1 (beta-site APP cleaving enzyme): Use of structure based design to convert a micromolar hit into a nanomolar lead. *J. Med. Chem.* **2007**, *50*, 4261–4264.
- (14) Rankovic, Z. CNS drug design: balancing physicochemical properties for optimal brain exposure. *J. Med. Chem.* **2015**, *58*, 2584–2608.
- (15) Oehlrich, D.; Prokopcova, H.; Gijsen, H. J. The evolution of amidine-based brain penetrant BACE1 inhibitors. *Bioorg. Med. Chem. Lett.* **2014**, *24*, 2033–2045.

- (16) Cumming, J. N.; Scott, J. D.; Li, Sarah W.; Cartwright, M.; Chen, X.; Cox, K.; Forman, M.; Gilbert, E. J.; Hodgson, R.; Hyde, L.; Jin, Y.; Kazakevich, I.; Kuvelkar, R.; Liang, X.; Mei, H.; Misiaszek, J.; Orth, P.; Stone, J.; Strickland, C.; Voigt, J. H.; Wang, H.; Werner, B.; Wong, J.; Parker, E. M.; Greenlee, W. J.; Kennedy, M. E.; Stamford, A. W. Discovery of MK-8931: a BACE inhibitor in phase 3 clinical development for Alzheimer's disease. In 249th ACS National Meeting & Exposition, Denver, CO, March 22–26, 2015, MEDI-246.
- (17) Hilpert, H.; Guba, W.; Woltering, T. J.; Wostl, W.; Pinard, E.; Mauser, H.; Mayweg, A. V.; Rogers-Evans, M.; Humm, R.; Krummenacher, D.; Muser, T.; Schnider, C.; Jacobsen, H.; Ozmen, L.; Bergadano, A.; Banner, D. W.; Hochstrasser, R.; Kuglstatter, A.; David-Pierson, P.; Fischer, H.; Polara, A.; Narquizian, R. β -Secretase (BACE1) inhibitors with high in vivo efficacy suitable for clinical evaluation in Alzheimer's disease. *J. Med. Chem.* **2013**, *56*, 3980–3995.
- (18) May, P. C.; Willis, B. A.; Lowe, S. L.; Dean, R. A.; Monk, S. A.; Cocke, P. J.; Audia, J. E.; Boggs, L. N.; Borders, A. R.; Brier, R. A.; Calligaro, D. O.; Day, T. A.; Ereshefsky, L.; Erickson, J. A.; Gevorkyan, H.; Gonzales, C. R.; James, D. E.; Jhee, S. S.; Komjathy, S. F.; Li, L.; Lindstrom, T. D.; Mathes, B. M.; Martenyi, F.; Sheehan, S. M.; Stout, S. L.; Timm, D. E.; Vaught, G. M.; Watson, B. M.; Winnroski, L. L.; Yang, Z.; Mergott, D. J. The potent BACE1 inhibitor LY2886721 elicits robust central $\text{A}\beta$ pharmacodynamic responses in mice, dogs, and humans. *J. Neurosci.* **2015**, *35*, 1199–1210.
- (19) Woltering, T. J.; Wostl, W.; Hilpert, H.; Rogers-Evans, M.; Pinard, E.; Mayweg, A.; Gobel, M.; Banner, D. W.; Benz, J.; Travagli, M.; Pollastrini, M.; Marconi, G.; Gabellieri, E.; Guba, W.; Mauser, H.; Andreini, M.; Jacobsen, H.; Power, E.; Narquizian, R. BACE1 inhibitors: a head group scan on a series of amides. *Bioorg. Med. Chem. Lett.* **2013**, *23*, 4239–4243.
- (20) Ginman, T.; Viklund, J.; Malmstrom, J.; Blid, J.; Emond, R.; Forsblom, R.; Johansson, A.; Kers, A.; Lake, F.; Sehgelmeble, F.; Sterky, K. J.; Bergh, M.; Lindgren, A.; Johansson, P.; Jeppsson, F.; Falting, J.; Gravenfors, Y.; Rahm, F. Core refinement toward permeable beta-secretase (BACE-1) inhibitors with low hERG activity. *J. Med. Chem.* **2013**, *56*, 4181–4205.
- (21) Tresadern, G.; Delgado, F.; Delgado, O.; Gijsen, H.; Macdonald, G. J.; Moechars, D.; Rombouts, F.; Alexander, R.; Spurlino, J.; Van Gool, M.; Vega, J. A.; Trabanco, A. A. Rational design and synthesis of aminopiperazinones as beta-secretase (BACE) inhibitors. *Bioorg. Med. Chem. Lett.* **2011**, *21*, 7255–7260.
- (22) Delgado, O.; Monteagudo, A.; Van Gool, M.; Trabanco, A. A.; Fustero, S. A practical entry to beta-aryl-beta-alkyl amino alcohols: application to the synthesis of a potent BACE1 inhibitor. *Org. Biomol. Chem.* **2012**, *10*, 6758–6766.
- (23) Cosner, C. C.; Markiewicz, J. T.; Bourbon, P.; Mariani, C. J.; Wiest, O.; Rujo, M.; Rosenbaum, A. I.; Huang, A. Y.; Maxfield, F. R.; Helquist, P. Investigation of N-aryl-3-alkylenepyrrrolinones as potential Niemann-Pick type C disease therapeutics. *J. Med. Chem.* **2009**, *52*, 6494–6498.
- (24) Viklund, J.; Kolmodin, K.; Nordvall, G.; Swahn, B. M.; Svensson, M.; Gravenfors, Y.; Rahm, F. Creation of novel cores for β -Secretase (BACE-1) inhibitors: a multiparameter lead generation strategy. *ACS Med. Chem. Lett.* **2014**, *5*, 440–445.
- (25) pK_a values calculated with ACD Labs Software v10; Advanced Chemistry Development Inc.: 110 Yonge Street, 14th Floor, Toronto, Ontario, Canada, MSC 1T4; <http://www.acdlabs.com/home/> (accessed August 10, 2015).
- (26) Wager, T. T.; Chandrasekaran, R. Y.; Hou, X.; Troutman, M. D.; Verhoest, P. R.; Villalobos, A.; Will, Y. Defining desirable central nervous system drug space through the alignment of molecular properties, *in vitro* ADME, and safety attributes. *ACS Chem. Neurosci.* **2010**, *1*, 420–434.
- (27) Groups at Novartis and Roche have recently patented morpholines with different substitution patterns: (a) Badiger, S.; Chebrolu, M.; Frederiksen, M.; Holzer, P.; Hurth, K.; Lueoend, R. M.; Machauer, R.; Moebitz, H.; Neumann, U.; Ramos, R.; Rueeger, H.; Tintelnot-Blomley, M.; Veenstra, S. J.; Voegtle, M. Oxazine derivatives and their use as BACE inhibitors for the treatment of neurological disorders. WO2011009943, 2011. (b) Badiger, S.; Chebrolu, M.; Hurth, K.; Jacquier, S.; Lueoend, R. M.; Machauer, R.; Rueeger, H.; Tintelnot-Blomley, M.; Veenstra, S. J.; Voegtle, M. Novel heterocyclic derivatives and their use in the treatment of neurological disorders. WO2012095469, 2012. (c) Badiger, S.; Chebrolu, M.; Frederiksen, M.; Holzer, P.; Hurth, K.; Li, L.; Liu, H.; Lueoend, R. M.; Machauer, R.; Moebitz, H.; Neumann, U.; Ramos, R.; Rueeger, H.; Schaefer, M.; Tintelnot-Blomley, M.; Veenstra, S. J.; Voegtle, M., Xiong, X. Oxazine derivatives and their use in the treatment of neurological disorders. WO2012006953, 2012. (d) Andreini, M.; Banner, D.; Guba, W.; Hilpert, H.; Mauser, H.; Mayweg, A. V.; Narquizian, R.; Power, E.; Rogers-Evans, M.; Travagli, M.; Valacchi, M.; Woltering, T.; Wostl, W. 3-Amino-5-phenyl-5,6-dihydro-2H-[1,4]oxazine derivatives, WO2011020806, 2011. (e) Andreini, M.; Gabellieri, E.; Narquizian, R.; Travagli, M.; Wostl, W. 1,4-Oxazines as BACE1 and/or BACE2 inhibitors. WO2012104263, 2012. (f) Andreini, M.; Gabellieri, E.; Guba, W.; Hilpert, H.; Mauser, H.; Mayweg, A. V.; Narquizian, R.; Power, E.; Travagli, M.; Woltering, T.; Wostl, W. 1,4-Oxazines as BACE1 and/or BACE2 inhibitors. WO2012098064, 2012.
- (28) Liao, C.; Nicklaus, M. C. Comparison of nine programs predicting pK_a values of pharmaceutical substances. *J. Chem. Inf. Model.* **2009**, *49*, 2801–2812.
- (29) Two tautomeric forms were considered in the calculation with ACD: one with endocyclic double bond, and one with exocyclic double bond. Performance of ACD on the training set was worse using an endocyclic double bonded NH tautomer (see Supporting Information). However, the endocyclic form is better for the final morpholine examples but still not as good as ADMET Predictor and introduces uncertainty of choosing the most appropriate tautomer.
- (30) Xu, Y.; Li, M. J.; Greenblatt, H.; Chen, W.; Paz, A.; Dym, O.; Peleg, Y.; Chen, T.; Shen, X.; He, J.; Jiang, H.; Silman, I.; Sussman, J. L. Flexibility of the flap in the active site of BACE1 as revealed by crystal structures and molecular dynamics simulations. *Acta Crystallogr., Sect. D: Biol. Crystallogr.* **2012**, *D68*, 13–25.
- (31) Please note the oxazine ring numbering reverses in the final compounds compared to the previous intermediates.
- (32) Tvaroska, I.; Carver, J. P. Ab-initio molecular-orbital calculation on carbohydrate model compounds 0.1. The anomeric effect in fluoro and chloro derivatives of tetrahydropyran. *J. Phys. Chem.* **1994**, *98*, 6452–6458.
- (33) Lee, S. S.; Greig, I. R.; Vocadlo, D. J.; McCarter, J. D.; Patrick, B. O.; Withers, S. G. Structural, mechanistic, and computational analysis of the effects of anomeric fluorines on anomeric fluoride departure in 5-fluoroxylosyl fluorides. *J. Am. Chem. Soc.* **2011**, *133*, 15826–15829.
- (34) Borghys, H.; Jacobs, T.; Van Broeck, B.; Dillen, L.; Dhuyvetter, D.; Gijsen, H.; Mercken, M. Comparison of two different methods for measurement of amyloid-beta peptides in cerebrospinal fluid after BACE1 inhibition in a dog model. *J. Alzheimer's Dis.* **2014**, *38*, 39–48.
- (35) Van Broeck, B.; Chen, J.-M.; Tréton, G.; Desmidt, M.; Hopf, C.; Ramsden, N.; Karra, E.; Mercken, M.; Rowley, A. Chronic treatment with a novel γ -secretase modulator, JNJ-40418677, inhibits amyloid plaque formation in a mouse model of Alzheimer's disease. *Br. J. Pharmacol.* **2011**, *163*, 375–389.
- (36) Sirius Analytical Ltd.: Forest Row Business Park, Station Road, Forest Row, East Sussex, RH18 SDW, UK; <http://www.sirius-analytical.com/> (accessed June 23, 2015).
- (37) Zhu, Z.; McKittrick, B.; Sun, Z.-Y.; Ye, Y. C.; Voigt, J. H.; Strickland, C.; Smith, E. M.; Stamford, A.; Greenlee, W. J.; Mazzola, R. D., Jr.; Caldwell, J.; Cumming, J. N.; Wang, L.; Wu, Y.; Iserloh, U.; Liu, X.; Huang, Y.; Li, G.; Pan, J.; Misiaszek, J. A.; Guo, T.; Le, T. X. H.; Saionz, K. W.; Babu, S. D.; Hunter, R. C.; Morris, M. L.; Gu, H.; Qian, G.; Tadesse, D.; Lai, G.; Duo, J.; Qu, C.; Shao, Y. Preparation of imidazolidin-2-imines and their analogs as aspartyl protease inhibitors for treating various diseases. WO2008103351A2, 2008.